VIENNA UNIVERSITY OF TECHNOLOGY
Institute of Chemical Engineering

# DIPLOMARBEIT

## Design and construction of an experimental setup to measure the impact of alkali metals on gasification

Ausgeführt zum Zwecke der Erlangung des akademischen Grades eines „Diplom-Ingenieurs“

unter der Leitung von

Univ.Prof. Dipl.-Ing. Dr.techn. Hermann Hofbauer

E166 Institut f. Verfahrenstechnik, Umwelttechnik und Technische Biowissenschaften

Eingereicht an der Technischen Universität Wien

Fakultät für Maschinenwesen und Betriebswissenschaften

von

Daniel Cenk Rosenfeld
1100669 (066 473)
Fünkhgasse 5A
3021 Pressbaum

Wien, im März 2017

_____
Daniel Cenk Rosenfeld

Ich habe zur Kenntnis genommen, dass ich zur Drucklegung meiner Arbeit unter der Bezeichnung

# Diplomarbeit

nur mit Bewilligung der Prüfungskommission berechtigt bin.

Ich erkläre weiters an Eides statt, dass ich meine Diplomarbeit nach den anerkannten Grundsätzen für wissenschaftliche Abhandlungen selbstständig ausgeführt habe und alle verwendeten Hilfsmittel, insbesondere die zugrunde gelegte Literatur genannt habe.

Des Weiteren erkläre ich, dass ich dieses Diplomarbeitsthema bisher weder im In- noch im Ausland (einer Beurteilerin/einem Beurteiler zur Begutachtung) in irgendeiner Form als Prüfungsarbeit vorgelegt habe und dass diese Arbeit mit der vom Begutachter beurteilten Arbeit übereinstimmt.

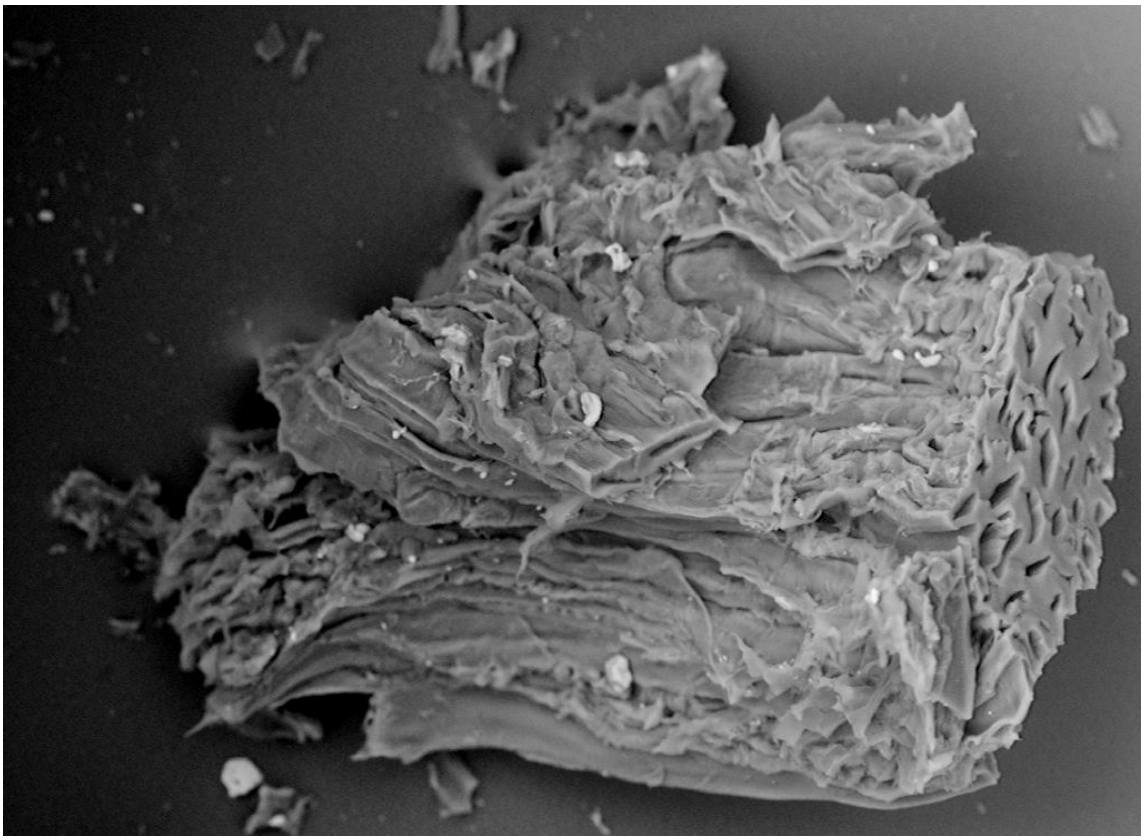

# Design and construction of an experimental setup to measure the impact of alkali metals on gasification

Master's thesis in Chemical and Process Engineering

Daniel C. Rosenfeld

Institute of Chemical Engineering
VIENNA UNIVERSITY OF TECHNOLOGY

Department of Energy and Environment
CHALMERS UNIVERSITY OF TECHNOLOGY

Gothenburg, Sweden 2017

Design and construction of an experimental setup to measure the impact of alkali metals on gasification



Master's Thesis 2017

Institute of Chemical Engineering
Vienna University of Technology
A-1040 Vienna
Austria

Department of Energy and Environment
Division of Energy Technology
Chalmers University of Technology
SE-41296 Gothenburg
Sweden

Cover:

A char particle in the SEM

Department of Energy and Environment
Gothenburg, Sweden 2017

**Design and construction of an experimental setup to measure the impact of alkali metals on gasification**

Daniel C. Rosenfeld
Department of Energy and Environment
Division of Energy Technology
Chalmers University of Technology

# Abstract

Biomass steam gasification is a promising way of producing synthetic gas that can be used for example in chemical industry and for fuel production. It can also be combined with heat and power generation and has a high potential as a renewable energy source. This has led to a lot of research about how catalytic active bed material could improve the quality of synthetic gas. Previous publications have shown that catalytic active bed material also has a positive effect on the efficiency of the char gasification reaction by transferring potassium from the bed material to the solid fuel.

The present work investigates the impact of different bed materials on steam gasification of char. This should help to analyse the role of alkali metals, especially of potassium, in char gasification. To examine this, a new fluidized bed system on lab scale has been designed and constructed, which allows for the execution of steam gasification experiments without the risk of an interaction between the reactor and the catalytic material. This has been done by performing steam gasification experiments of char in active and nonactive olivine as bed material. After 50% conversion, the char has been analysed with a SEM/EDX.

It was found that the activated olivine has a strong catalytic effect on the steam gasification of char. This results in a higher reaction rate and a reduction by 50% of the conversion time. Further experiments have shown that this effect is decreasing over time. The char analysis has shown that the potassium was transferred from the bed material to the fuel.

# Kurzfassung

Biomasse-Dampfvergasung ist eine der vielversprechendsten Methoden der Synthesegasherstellung, welche zum Beispiel in der chemischen Industrie oder in der Brennstoffproduktion verwendet wird. Sie kann mit Wärme- und Energieproduktion gekoppelt werden und hat ein hohes Potential als erneuerbarer Energieträger. Dieses Potential hat zu umfangreichen Forschungsarbeiten geführt, welche sich damit beschäftigen wie katalytisch aktives Bettmaterial die Qualität des Synthesegases verbessern kann. Frühere Publikationen haben gezeigt, dass katalytisch aktives Bettmaterial einen positiven Effekt auf die Effizienz der Kohlevergasungsreaktion hat, indem Kalium vom Bettmaterial zum festen Brennstoff transferiert wird.

Die vorliegende Arbeit untersucht den Einfluss verschiedener Bettmaterialien auf die Dampfvergasung von Kohle. Die Rolle der Alkalimetalle, im Speziellen jene von Kalium, wurde im Hinblick auf die Kohlevergasung analysiert. Um das zu untersuchen wurde ein neues Wirbelschichtsystem im Labormaßstab konstruiert. Damit konnten Dampfvergasungsexperimente durchgeführt werden, ohne das Risiko einzugehen, dass der Reaktor mit dem katalytischen Material wechselwirkt. Das wurde mittels Dampfvergasungsexperimenten von Kohle in aktivem und nicht-aktivem Bettmaterial gemacht. Nach 50% Umsatz wurde die Kohle mit SEM/EDX analysiert.

Es zeigte sich, dass das aktive Olivin einen starken katalytischen Effekt auf die Dampfvergasung von Kohle hat. Dies konnte anhand der hohen Reaktionsrate und einer Reduktion der Reaktionszeit um 50% geschlussfolgert werden. Der katalytische Effekt nimmt mit der Zeit ab. Die Analyse der Kohle hat ergeben, dass das Kalium vom Bettmaterial zum Brennstoff transferiert wurde.

# Acknowledgements

I would like to express my most sincere gratitude to my main supervisor at the Vienna University of Technology, Prof. Hermann Hofbauer for giving me the possibility to write my master thesis in Gothenburg and for introducing me to the field of biomass gasification.

I would also like to thank my examiner Asst. Prof. Martin Seemann and my supervisor Teresa B. Vilches for giving me the opportunity to work on an exciting project and the always enthusiastic supervision. Your constructive inputs have always helped me to write this work.

A very big thank you to Pavleta Knutsson, Jessica Bohwalli and Sébastien Pissot for providing the materials that I needed to build the setup and to Oscar Gründer and Jutta Stutzmann for the discussion and feedback after my presentation.

Thanks to Stefan Müller and Johannes C. Schmid for your advice which you gave me before I started the work in Gothenburg.

To my friends, Alex, Gabriel, Niki, Lucy and Vanessa and my parents for supporting me during my ERASMUS+ semester and to my CIRC group, it was always a pleasure to play volleyball and philosophize about pineapples together.

Thank you also to the people who supported me during my studies and the work of my master thesis.

Finally, and most of all, to my beloved Catherine for your invaluable support received over the years. It was always good to have someone to talk with about everything.

Daniel C. Rosenfeld, Göteborg 2017

# Notation

## Abbreviations

| | |
|---|---|
| CEM | controlled-evaporator-mixer |
| EDX | energy dispersive x-ray |
| LFM | liquid-flow-controller |
| MFC | mass-flow-controller |
| SEM | scanning electron microscopy |
| TGA | thermogravimetric analyser |
| Ar | Archimedes number [-] |

## Symbols

| | |
|---|---|
| $d_i$ | inner diameter [m] |
| $d_o$ | outer diameter [m] |
| $d_{sv}$ | sauter mean diameter [m] |
| g | gravity acceleration [m/s²] |
| ΔH | enthalpy difference [kJ/mol] |
| $H_B$ | bed height [m] |
| $H_R$ | reactor height [m] |
| Mc | molar mass of carbon [g/mol] |
| $m_c$ | converted time of carbon [kg] |
| $m_{total}$ | total amount of carbon [kg] |
| p | pressure [Pa] |
| R | gas constant [J $mol^{-1}$ $K^{-1}$] |
| r | reaction rate [s-1] |
| $r_w$ | average conversion rate [$s^{-1}$] |
| T | Temperature [K] |
| $U_M$ | velocity in the metal reactor [m/s] |
| $U_{mf}$ | minimum fluidization velocity [m/s] |
| $U_Q$ | velocity in the quartz glass reactor [m/s] |
| $\dot{V}_{gas}$ | gas flow [m³/s] |
| $X_C$ | carbon conversion [-] |
| x | molar fraction [-] |
| ε | void fraction [-] |

$\rho_g$ gas density [kg/m³]

$\rho_P$ particle density [kg/m³]

$\mu$ dynamic viscosity [Pa s]

# Contents

# 1 INTRODUCTION

## 1.1 MOTIVATION

In the past centuries, the industrialization has led to a massive increase in the demand of energy. The answer of the 20th century was fossil fuels. The fossil fuels and the still increasing demand of energy has led to the problem of climate change that we are facing now. It is necessary to create possibilities of energy production without increasing the amount of greenhouse gases in the atmosphere. Otherwise it would not be possible to maintain the climate change on a level that is still manageable [1], [2].

Therefore and because of the geographic location, the energy production from biomass and hydropower has gained more importance. This is the reason for the increasing amount of energy produced by alternative sources including biomass. Hydropower is of insufficient capacity for the steadily increasing demand of energy. [3], [4].

Biomass provides the possibility for producing energy and secondary fuels on a climate neutral basis. This means that biomass could be one of the best-known possibilities for producing energy without the problem of the greenhouse gas effect. It also provides a possibility in terms of waste management. Thus, side products in the food production that are composted could be used in biomass plants [2].

The biggest problem of biomass energy and fuel production is the efficiency and therefore its economic rentability. This has led to the development of power plants that are based on gasification which are combined with heat and power generation [5]. An additional possibility of improving the efficiency is to use a catalytic active bed material, e.g. the alkali and alkali earth metals. This could also lead to a higher quality of the synthetic gas [6].

In order to increase the efficiency, the Vienna University of Technology and Chalmers University of Technology dedicated a lot of research on biomass-steam gasification in dual fluidized bed systems. In dual fluidized bed systems, the necessary heat for the gasification reactor is provided by a separate combustion reactor. The biomass is gasified with steam. The bed material used as the heat carrier in the dual fluidized bed system in Vienna is olivine. It is possible to produce a high-quality biogas with this system without needing pure oxygen as gasification agent or a high temperature heat carrier. The produced biogas can be used as an alternative to natural gas [7], [8].

## 1.2 AIM AND STRUCTURE OF THE THESIS

The goal of the thesis is to investigate the impact of different bed materials on steam gasification of biomass. It is therefore necessary to build a setup to investigate the impact of alkali metals on gasification in different gas environments. The essential tasks of the creation process are defining the testing procedure and the data evaluation framework

The thesis is divided into three parts. The first part describes the theory about fluidized bed steam gasification. It should give a short overview of the possibilities of gasification and in fluidized bed reactors. The second part should show a schematic of the system design and which of its components differ from other pre-existing systems that have already been used. It also contains the information about the experimental setup and defines the method of evaluation of the data gathered during experiments with the setup. In the third part of the study, the evaluated data will be explained and discussed.

# 2 THEORETICAL BACKGROUND

## 2.1 FLUIDIZED BED

Fluidized bed describes a reactor in which a bulk of small particles is transformed into a state where it acts like a fluid. The effect which occurs in fluidized beds is called fluidization. Fluidization is achieved by sending a gas flow with a certain velocity to the reactor. The gas flow enters the reactor from the bottom and must have a velocity that is at least as high as the so called minimum fluidization velocity ($U_{mf}$) [9]. There are several empirical equations for $U_{mf}$. For fine particles, Wen and Yu defined it as [10]:

$$U_{mf} = \frac{\mu}{\rho_g \, d_{sv}} \left[ \sqrt{33.7^2 + 0.0408 * Ar} - 33.7 \right]$$

*Eq. 2-1*

With [11]

$$Ar = \frac{\rho_g \, d_{sv}^3 \left( \rho_p - \rho_g \right) g}{\mu^2}$$

*Eq. 2-2*

μ … Dynamic viscosity [Pa*s]

$\rho_g$ … Gas density [kg/m³]

$\rho_p$ … Bed particle density [kg/m³]

$d_{sv}$ … Sauter mean diameter [m]

Ar … Archimedes number [-]

g … Gravity acceleration [m/s²]

There are many ways to characterise particles by their diameter. Most of the commonly used calculations are using the Sauter mean diameter $d_{sv}$. It is described as the diameter of a spherical object with the same volume-to-surface ratio as the particle [12].

One of the common used characteristics of fluidized beds is the pressure drop $\Delta p$. It is defined as [13]:

$$\Delta p = (1 - \epsilon)\left(\rho_p - \rho_g\right) g\, H_B$$

*Eq. 2-3*

ε … Void fraction at minimum fluidization [-]
$H_B$ … Height at fluidization point [m]

The void fraction at minimum fluidization $\varepsilon$ is defined as the ratio between the void volume and the total volume of the bed [14].

Some of the advantages of fluidized beds are the good mixing, mass transfer, and heat transfer abilities. There are various physical and chemical processes where fluidized beds can be used. Some of the chemical processes are listed in Table 1 [3].

*Table 1: Examples of chemical processes with fluidized beds*

| Solid as heat carrier | Solid as catalyst | Solid as reaction partner |
|---|---|---|
| Pyrolysis | Catalytic cracking | Ore roasting |
| Gasification | Fischer-Tropsch process | Ore reduction |
| Combustion | Acrylnitrile production | Calcination |
| | Methane production | |

### 2.1.1 Geldart classification of particles

One of the most common ways to classify a fluidized bed is to categorize the bed material by its ability to fluidize. The common method of particle classification is the one by Derek Geldart. He classified particles into four different groups [15]:

- Group A: The particle size and the particle density is very low. This fluidized bed expands when reaching the fluidization point before it starts building bubbles. The reason for the expansion is that the bed materials of this group are still influenced by cohesive forces.
  Most of the commercially operated cracking plants are using catalysts from this group.

- Group B: It contains bed materials with a Sauter mean diameter between 40 µm and 500 µm. Bed materials of this group are bubbling right after reaching the minimum fluidization conditions, because of the missing influence of cohesive forces.
  Because of bubbling right after reaching the fluidization point without much expansion, materials of this group have good mixing ability.
  Group B particles are the commonly used type of particles in thermochemical conversion of solid fuels. This leads to an important role in fluidized bed technologies.

- Group C: Particles of this group are small and hard to fluidize. This difficult fluidizability comes from the strong influence of the cohesive forces. In this case the cohesive forces on the particles are much higher than the forces that occur due to the fluidizing gas.
  Bed materials of this group are rarely used in fluidized bed technologies.

- Group D: Big and dense particles are part of this group.
  They are mostly used in the food industry (e.g. coffee beans).

Figure 1 shows a diagram for the classification of bed materials by Geldart.

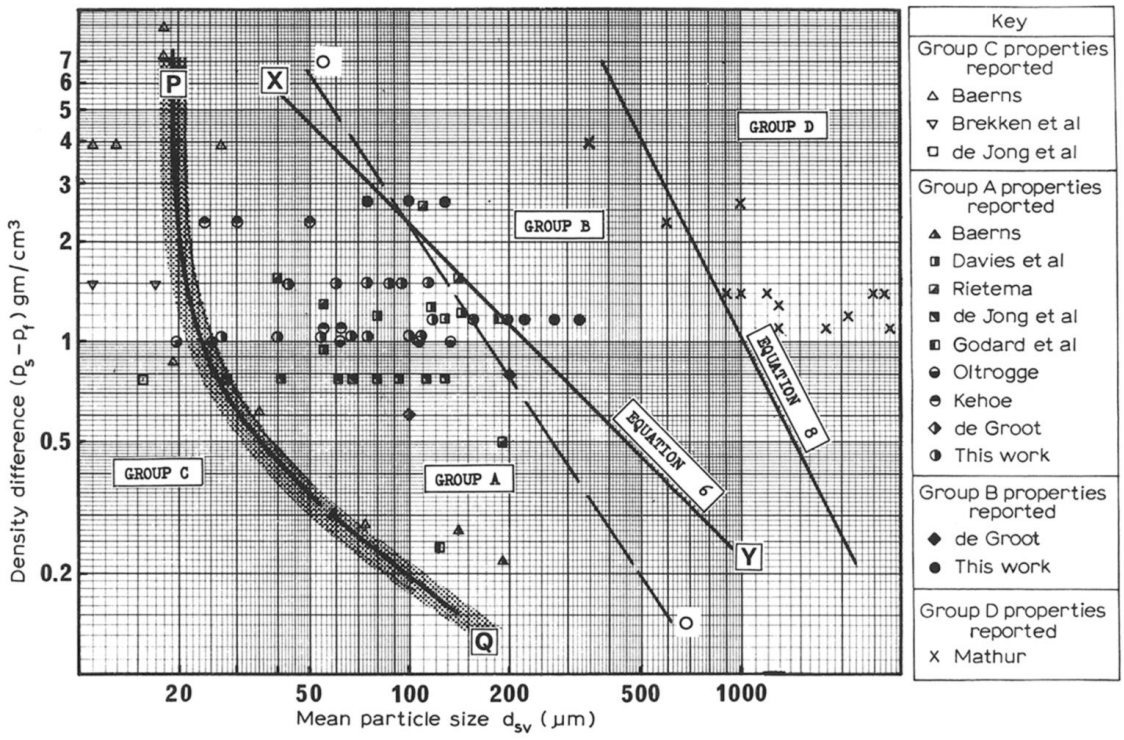


*Figure 1: Powder classification diagram for fluidization by air [15].*

## 2.2 THERMOCHEMICAL CONVERSION OF BIOMASS

Thermochemical conversion of biomass occurs as a result of an impact of heat and/or chemical reactions. It transforms large molecules into smaller ones. The types discussed in this thesis will be pyrolysis, combustion, and gasification. Of the three types of thermochemical conversion, the focus will be on the gasification process.

### 2.2.1 The pyrolysis

Pyrolysis is a pre-step of thermochemical conversion that takes place in combustion as well as in gasification. Pyrolysis describes the thermal process in which the volatiles are leaving the wood in the form of hydrocarbons – $H_4$, $CO$, etc. [16].

Pyrolysis can be used to provide liquid or solid secondary fuels (char, biodiesel, etc.). [17] The main method for producing char with a pyrolysis process is called carbonization. It is a process at temperatures above 500 °C without any oxygen. Normally an inert environment ($N_2$-atmosphere) is provided for the process. During the process, biomass is first dried and in a second step pyrolyzed [18].

### 2.2.2 Combustion

Combustion is the type of thermochemical conversion mostly applied on commercial scale and is probably the oldest one. The chemical reaction of combustion is [19]:

$$C_aH_bO_c + (a + \frac{b}{4} - \frac{c}{2})O_2 \rightarrow aCO_2 + \frac{b}{2}H_2O$$

*Eq. 2-4*

The combustion of biomass proceeds through the following steps [20]:

1. Heating of the fuel
2. Drying of the fuel
3. Pyrolytic decomposition of the biomass due to the heat impact
4. Gasification of the solid carbon to CO with $CO_2$, steam and $O_2$
5. Oxidization of the combustible gases as shown in Eq. 2-4 at high temperatures (700 °C to 1500 °C)
6. Heat transfer from the flame to the newly added fuel

Combustion is used in various systems. It can be used to combust fuel in a fireplace to provide heat for a home, in a commercial combustor to produce heat which can be used to produce electricity, provide energy for reactions, etc. In dual fluidized bed gasification systems, it is used to provide heat for the gasification reactor. Figure 2 shows a schematic for the combustion in a fluidized bed system [21].

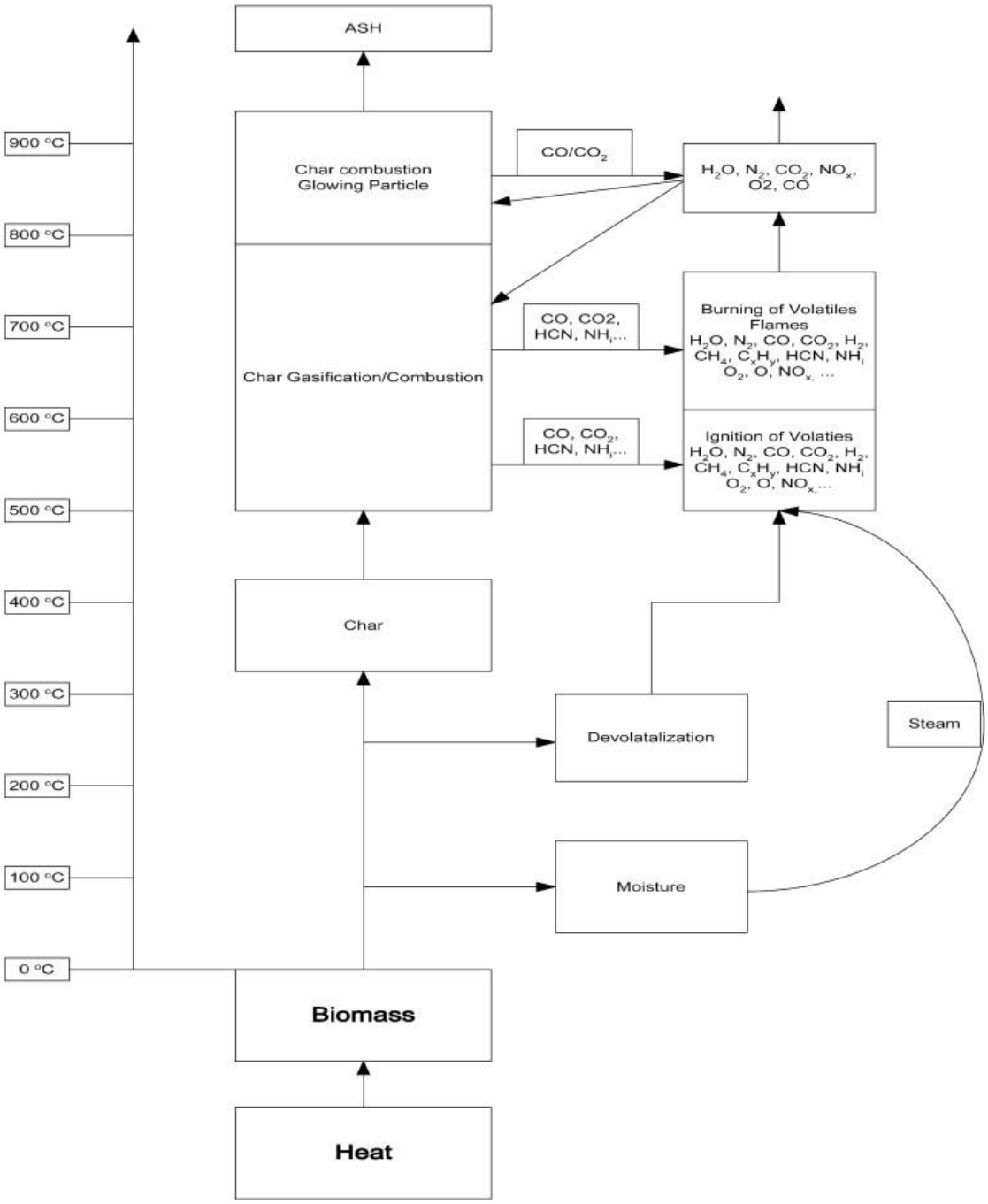


*Figure 2: Schematic of a combustion process in a fluidized bed system [21].*

### 2.2.3 The gasification process

The gasification process converts solid fuel into CO, $CO_2$ and $H_2$ at high temperatures and in the presence of a gasification agent. The main difference between combustion and gasification is the controlled amount of oxygen and/or steam. The gasification reactions can be described as follows [22], [23]:

$$C + H_2O \rightarrow CO + H_2 \quad \Delta H = +131 \text{ kJ/mol}$$

*Eq. 2-5*

$$C + CO_2 \rightarrow 2CO \qquad \Delta H = +172 \text{ kJ/mol}$$

*Eq. 2-6*

Both processes are endothermic. This leads to a high amount of heat development, which is necessary for the reactions to take place. One reaction that goes along with a gasification process with steam, is the water gas shift reaction. This reaction is an important gas phase reaction in steam gasification systems [23].

$$CO + H_2O \leftrightarrow CO_2 + H_2 \qquad \Delta H = -41 \text{ kJ/mol}$$

*Eq. 2-7*

The gasification process can be characterized by the degree of carbon conversion $X_C$, the rate of carbon conversion $r_w$ and the instantaneous reaction rate $r$ [22]. A typical value for $r$ in a non-catalytic gasification process is around 0.001 $s^{-1}$ [24], [25].

A study by Capucine Dupont has shown that, within the range of 800°C to 1000°C, at a pressure of 1 bar and with wood as the biomass, the limiting step of the gasification process is the chemical reaction Eq. 2-5 and that the only way of increasing the gasification rate is to increase the temperature. The particle size does not influence the rate of conversion [26].

## 2.3 BED MATERIALS

The main function of the bed material in a fluidized bed is to transfer heat. Beyond its ability to transfer heat, different bed materials can also have catalytic effects on a chemical process. Choosing the right bed material, it is always necessary to consider the following properties [6]:

### Chemical properties

The chemical properties are of high importance in gasification processes. In gasification, the bed material has a high impact on the quality, properties and composition of the produced gas. This follows mainly from the catalytic impact of the bed material. If the bed material has no catalytic effect on the gasification process, the produced gas would not be of as high quality as with a catalytic bed materials [6]. For example, silica sand is a non-active/inert bed material, while dolomite and alkali-based bed materials are active [23], [27]. It is possible to activate non-active bed materials by mixing active materials into them. There are many ways to activate bed materials, e.g. enriching olivine with nickel [28], or adding salts like $K_2CO_3$ [29].

### Mechanical properties

The particles in a fluidized bed have to withstand thermal stress and mechanical impact. The resulting degradation leads to a decrease in particle size and mass, which changes the fluidization properties and process conditions. Because of the loss of fine material due to entrainment, it is normally necessary to add bed material after some time [30].

### Economical properties

The economical properties are of most importance when it comes to finalizing a large-scale plant. Bed materials used in large-scale plants must

show a good balance between its chemical and mechanical advantages and with the price of the raw material [6].

### 2.3.1 Olivine as bed material

Different bed materials have been used in fluidized bed gasifiers, e.g. silica sand, dolomite, olivine, bauxite, ilmenite, and feldspar [31], [32]. The one that was used for the experiments of this thesis was olivine. It is a cheap bed material that can be found inside the upper earth mantle. One problem that can be caused by activated olivine is that it can contain heavy metals like Ni which possibly leads to environmental damage as a result of the disposal of the bed material [33].

Olivine is a bed material based on magnesium oxide and silicon dioxide. Publications have shown, that even with the active materials (e.g. Fe) inside the olivine, it has not shown an effect as big as expected on the gasification process [29], [34].

There are various methods of activating bed material. For example, one method performed at Chalmers University of Technology, is the addition of S and $K_2CO_3$ to the bed material during the experiments in the dual fluidized bed unit [29]. Another activation method is e.g. calcinating the olivine [28].

## 2.4 ALKALI-METALS

Alkali metals are the metals in the first group of the periodic system. These elements are Lithium, Sodium, Potassium, Rubidium, Caesium and Francium. Alkali metals are part of the fuel composition that are used in gasification processes.

### 2.4.1 The impact of alkali metals on the gasification process

Alkali metal salts have shown a positive catalytic effect on the char gasification process. The most catalytic of alkali compounds that were investigated in gasification research are the oxides, hydroxides and carbonates [35]. Previous experiments have shown that in the group of alkali metal carbonates, $K_2CO_3$ has the biggest catalytic effect on char gasification out of all of them [36]. This is the reason why $K_2CO_3$ was chosen for the activation of the bed material (please refer to Chapter 2.3.1) [37].

### 2.4.2 Potassium as catalyst during char-steam gasification

In a steam gasification process the $K_2CO_3$ reacts in the following way according to the research of Wang J. [25]:

$$K_2CO_3 + C \rightarrow K_2O + CO_2 + C \rightarrow 2K + CO_2 + CO$$

*Eq. 2-8*

$$2K + 2nC \rightarrow 2KC_n$$

*Eq. 2-9*

$$2KC_n + 2H_2O \rightarrow 2nC + 2KOH + H_2$$

*Eq. 2-10*

$$2KOH + CO_2 \rightarrow K_2CO_3 + H_2O$$

*Eq. 2-11*

### 2.4.3 Potassium catalysts in a quartz glass reactor

For investigations of reactions at elevated temperatures, quartz glass is a common material used as reactor material due to its high temperature resistance and relatively inert behaviour. However, alkali metals and $SiO_2$ are possible reaction partners at high temperatures. On the available reactor systems at 900 °C, this is also visible in the form of a white deposition on the inside of the reactor wall after cooldown. Reactions between alkali carbonates and $SiO_2$ can be described by [38]:

$$Me_2CO_3 + nSiO_2 \rightarrow M_2O * nSiO_2 + CO_2$$

*Eq. 2-12*

The Me describes the alkali metal. In case of $K_2CO_3$ it would react in the following way:

$$K_2CO_3 + SiO_2 \rightarrow K_2SiO_3 + CO_2$$

*Eq. 2-13*

$K_2SiO_3$ is also known as potassium metasilicate [39].

To get information on the impact of alkali metals on the gasification process, it is necessary to provide an environment which does not interact with the alkali metals. However, because of the likely interaction between K (or any other alkali metal) and $SiO_2$, quartz glass is not a viable reactor material. For this reason a metal reactor was installed for this work.

# 3 METHODOLOGY AND EXPERIMENTAL SETUP

The experiments were performed in two different types of reactors. They were made of quartz glass and steel respectively. There was no difference in the gas supply, gas conditioning and analysis system, except for the additional 100 mLn/min $N_2$ introduced through the fuel-feeding-system of the metal reactor as purge gas. The additional $N_2$ from the top of the reactor should not have an impact on the gasification process of the char. Only a small change in the evaluation of the data was necessary.

## 3.1 EXPERIMENTAL SETUP OF A FLUIDIZED BED REACTOR

The whole setup for the experiments consists of five main parts. The steam generator, the reactor, the oven, the cooling system, and the analyser. A schematic of the system is provided in Figure 3.

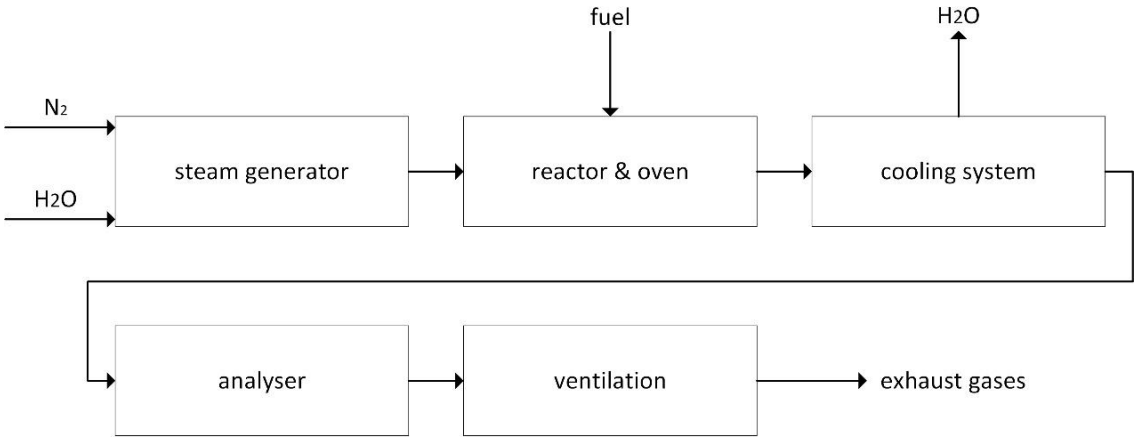


*Figure 3: Schematic of the setup for the experiments*

### 3.1.1 Steam generator

Main parts of the steam generator are the vessel for the water, the liquid-flow-controller (LFM), the mass-flow-controller (MFC), and the controlled-evaporator-mixer (CEM). After filling the vessel with distilled water and opening the valves V1 and V2, the water-supply-system is under pressure and ready for operation. Because of the $N_2$ the vessel is under pressure and the water can be pumped out through the valve V3 and the LFM directly to the CEM. The LFM can handle up to 30 g of $H_2O$ per hour.

When the valves V5 and V6 ore opened, the $N_2$ also reaches the MFC. The MFC can handle gases up to 500 mLn/min. After setting a constant liquid- and gas-flow with the LFM and MFC the CEM mixes the two phases and heats the mixture up to the temperature where it reaches a homogenous gas phase. The schematic of the steam-generator is shown in Figure 4.

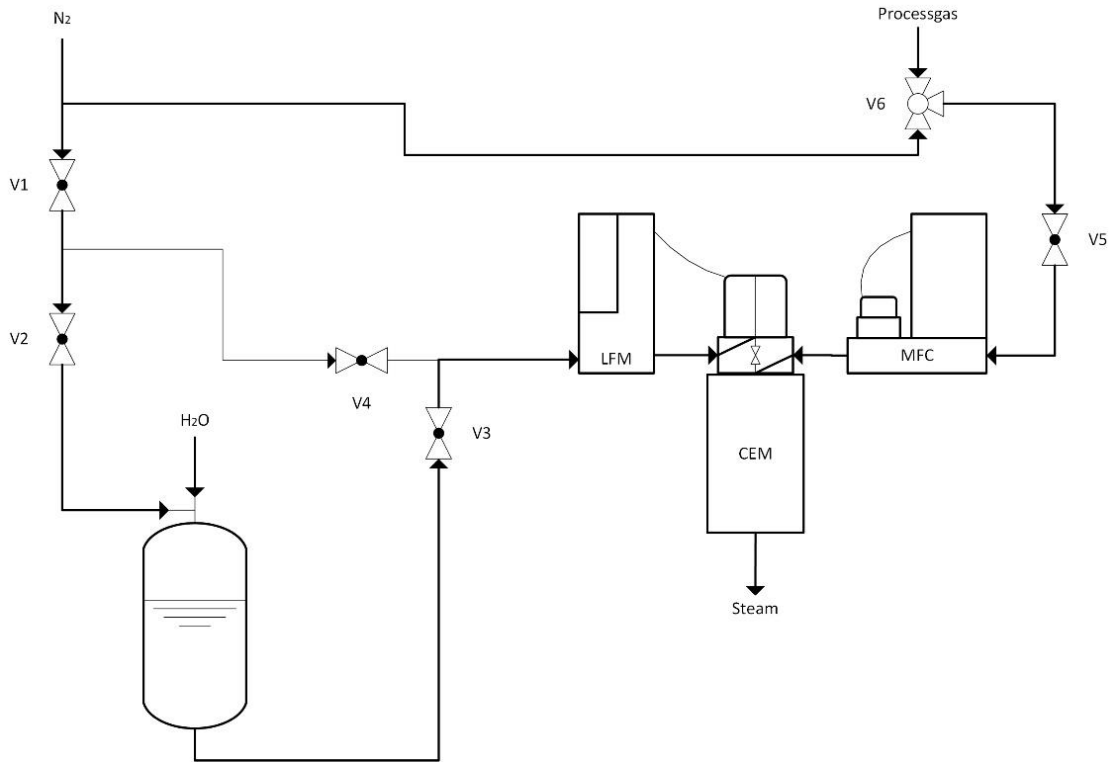


*Figure 4: Schematic of the steam-generator*

During all the experiments the MFC was set to 500 mLn/min of $N_2$ and the LFM to 18 g/min. The 18 g/min setting corresponds to 400 mLn/min of steam. So, all the experiments had a fluidization with 900 mLn/min of a steam-nitrogen mixture with 44.4% of steam.

### 3.1.2 Reactor and oven

Both, the metal and the quartz glass reactor were set inside a vertical split tube furnace which can reach temperatures of up to 1200 °C. Normally in dual fluidized bed gasification, the heat in the gasification reactor is provided by a combustion reactor over the circulating bed material. But in a lab scale model it is not necessary to have a dual fluidized bed when it comes to the analysis of the gasified char, the used bed material, or the impact of alkali metals. The extra combustion reactor in a dual fluidized bed should not change the conditions of the gasification process in a way that has an impact on the analysed parameters or objects. So, it is much easier to provide the heat by an external furnace.

Only two values were measured directly inside the reactor: the pressure difference and the temperature. To obtain the pressure difference between the entering and the exiting gas, two pressure measuring units were set, one before and one after the reactor. The pressure difference is important in order to obtain information about the fluidization of the bed material. As already mentioned in Chapter 2.1, there is always a pressure drop in fluidized beds. In the case of the metal reactor as well as the non-transparent reactor mantle, because of the oven, the pressure difference is the only measurable quantity or visual effect that indicates that the bed material is fluidized.

The temperature was measured by a thermocouple placed inside the bed material at the head of the reactor. The reason is that the char is in the bed material.

All pipes that direct the steam to the reactor or the exhaust gas to the cooling system are wrapped with heating bands and in insulation to prevent water condensation in the pipes.

### Quartz reactor

Table 2 shows the basic dimensions of the quartz glass reactor.

*Table 2: Dimensions of the quartz glass reactor*

| $d_o$ | $d_i$ | $H_B$ | H |
|---|---|---|---|
| 24 mm | 23 mm | 29 mm | 400 mm |

The first experiments were carried out inside a quartz glass reactor. It is made out of three pieces - the head, the reactor itself, and the bottom. The reactor was connected to the whole system through a metal connection with a sealing ring at the gas inlet and gas outlet tube. The fuel feeding system was made of a teflon connector, a shrinking tube, and a hose clip. Figure 5 shows an image of the quartz reactor before it is set inside the furnace.

*Figure 5: Quartz glass reactor before setting it into the system*

### Metal reactor

Table 3 shows the basic dimensions of the metal reactor.

*Table 3: Dimensions of the metal reactor*

| $d_o$ | $d_i$ | $H_B$ | H |
|---|---|---|---|
| 48 mm | 42 mm | 8.7 mm | 425 mm |

As shown in Figure 6 the three parts of the metal reactor are connected as a flange with four screws. The top part of the reactor consists of a lid with three 6 mm pipes – connected to a thermocouple, the gas outlet and the pressure measurement – and one 10 mm pipe – for the fuel feeding system.

*Figure 6: Metal reactor before setting it into the system*

Compared to the quartz reactor, beside the metal reactor being made out of a different material, steel instead of quartz, its diameters and fuel feeding systems are also different. It is possible to feed the reactor with larger particle sizes or even with whole pellets, with the fuel feeding system – as long as the outer diameter of the pellets is not too large for the 10 mm pipes that are used to connect the different parts. Another difference to the quartz glass setup is the $N_2$ supply at two different points of the fuel feeding system, to avoid problems with moisture or condensed water. The pipes below the bottom valve of the fuel feeding system are also wrapped in insulation to reduce the risk of moisture and condensed water.

Figure 7 shows the schematic of the used system:

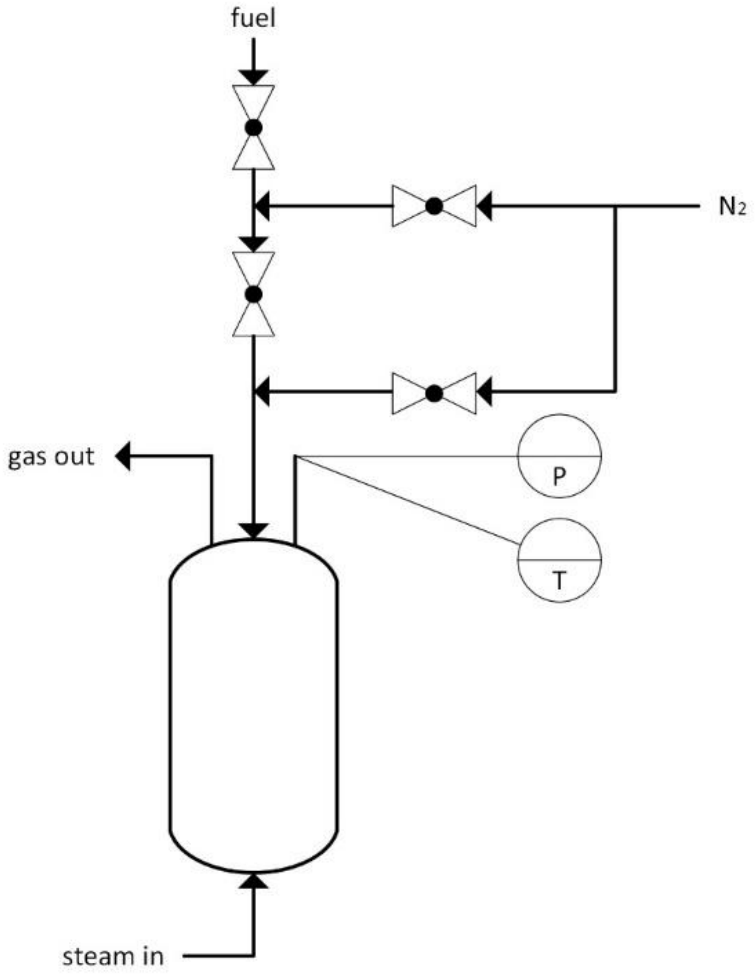


*Figure 7: Schematic of the metal reactor*

### 3.1.3 Cooling system and analyser

Before entering the analyser, it is necessary that the gas is free from $H_2O$. Otherwise it would damage the gas flow measurement or even the gas detector of the analyser. Because of that, the exhaust gases of the reactor first have to pass the cooling system first (M&C ECP 3000). The exhaust gas of the reactor passes the cooling system through two screw tops with a pipe in the middle. Figure 8 shows an image of the cooling system.


*Figure 8: Image of the cooling system used in the experimental setup to cool down the exhaust gas to 5 °C (M&C ECP 3000).*

After passing the cooling system, the gas temperature should be at +5 °C and all the $H_2O$ has accrued to a pipe at the bottom.

The analyser used in the system is an NGA 2000 MLT 4 from EMERSON. It measures the flow of the gas in mLn/min and the concentrations of $CH_4$, CO, $CO_2$, $H_2$, and $O_2$ in the exhaust gas. For measuring the gas concentrations, the analyser has two built-in photometers. One to measure $H_2$ and $O_2$ and the other to measure $CH_4$, CO, and $CO_2$. While the gas is passing the analyser, the photometers send and detect a light impulse and measure the wavelength. The wavelength is then used for calculating the percentages of the specific gases.

It is necessary to calibrate the analyser to obtain accurate readings of gas composition. This is done in two steps. The first step is to do a zero calibration by sending a flow of pure $N_2$ to the analyser and setting all the measured gases to zero. The second step is the span calibration. The span calibration uses a gas of a known gas composition ($CH_4$ = 25%, CO = 20%, $CO_2$ = 40% and $H_2$ = 15%) that is programmed into the gas analyser.

After passing the analyser, the exhaust gas is led to the ventilation.

## 3.2 MATERIALS

The experiments were carried out using char out of wood pellets in two different types of olivine bed materials – an unused and an activated one.

### 3.2.1 Biomass char

The char for the experiments was produced in a thermogravimetric analyser (TGA). With the TGA, wood pellets were heated up in two steps in a nitrogen atmosphere.

The first step is to dry the wood pellets. With a rate of 16 °C/min the char was heated up from 25 °C to 130 °C where it was held for ten minutes. The second step is to devolatilize the pellets. With a rate of 49 °C/min the char was heated up to 915 °C where it was held for 7 minutes.

Table 4 shows the composition of the wood pellets that were used to produce the char for the experiments.

*Table 4: Composition of the original wood pellets in %*

| Ash | Carbon | Hydrogen | Nitrogen | Sulfur | Chlorine | Oxygen |
|---|---|---|---|---|---|---|
| 0.4% | 50.4% | 6.1% | 0.06% | <0.01% | 0.01% | 43.0% |

Each experiment was performed with 0.4 g of fuel. The char for the experiments in the quartz glass reactor was crushed and sieved in fractions mentioned in Chapter 3.3.1. The length of the char pellets for the experiments in the metal reactor, mentioned in Chapter 3.3.1, was measured with a slide gauge.

### 3.2.2 Bed material

Two different bed materials were used in this work: unused olivine and activated olivine. The activated olivine is a bed material sample from the Chalmers gasifier which has been activated by adding S and $K_2CO_3$ to the bed material during the experiments in the dual fluidized bed unit at Chalmers (see Chapter 2.3.1).

Table 5 shows the composition of the unused olivine for the experiments.

*Table 5: Composition of unused olivine in %*

| | | | |
|---|---|---|---|
| MgO | 49.6% | $Al_2O_3$ | 0.46% |
| $SiO_2$ | 41.7% | NiO | 0.32% |
| $Fe_2O_3$ | 7.4% | $Cr_2O_3$ | 0.31% |

The unused olivine as well as the activated olivine were sieved to get 15 g fractions of 125 µm to 180 µm. With the fraction size and the following characteristics $\rho_s$ = 3.2 g/cm³ (density of the bed material) and $\rho_g$ = 0.025 g/cm³ (density of the fluidizing gas) one can derive from Figure 1, that the bed material is classified as Geldart group B.

## 3.3 GASIFICATION OF WOODEN CHAR

All experiments were carried out with the same type of char under similar experimental conditions. The only differences between the two setups were the diameters of the reactor, height of the bed, the extra nitrogen from the fuel feeding system of the metal reactor, and the particle size of the used char.

Table 6 shows the operating conditions of the gasification process that are the same in both cases:

*Table 6: Operating conditions during the char gasification tests with both reactors*

| | |
|---|---|
| Gas flow | 900 mLn/min |
| Amount of steam in the fluidizing gas | 44.4% |
| Temperature of the bed material | 900 °C |

In both cases, the bed material was added before setting the reactor into the system. The bed was fluidized with $N_2$ during the heating. Once the final temperature of 900 °C was reached, steam was added. When the flows were stable, the char particles were fed from the top of the reactor via the fuel feeding system.

*Table 7: Parameters for $U_{mf}$ and $\varepsilon$ calculation*

| $d_{sv}$ | $\rho_p$ | $\rho_g$ | $\mu$ |
|---|---|---|---|
| 152.5 µm | 3200 kg/m³ | 0.249 kg/m³ | $4.4*10^{-5}$ Pa*s |

Out of Eq. 2-1 and Eq. 2-2 follows with the parameters of Table 2, Table 3 and Table 7:

*Table 8: Values for $U_{mf}$ and Ar*

| Ar | $U_{mf}$ |
|---|---|
| 22.95 | 0.016 m/s |

The exact calculation can be found in Appendix B.

### 3.3.1 Overview of the experiments

Table 9 shows an overview of the experiments that were carried out with the quartz glass reactor and the metal reactor.

*Table 9: Overview of all the experiments included in this thesis*

| | Reactor | Olivine | Fuel type | Fuel size | Conversion | Comment |
|---|---|---|---|---|---|---|
| 1 | Quartz | Unused | Pellets | 5 mm length | Full | Unsuccessful |
| 2 | Quartz | Unused | Particle | 125 µm – 180 µm | Full | Unsuccessful |
| 3 | Quartz | Unused | Particle | 500 µm - 710 µm | Full | |
| 4 | Quartz | Activated | Particle | 500 µm – 710 µm | Full | |
| 5 | Metal | Unused | Pellets | 10 mm length | Full | |
| 6 | Metal | Unused | Pellets | 7 mm length | Full | Unsuccessful |
| 7 | Metal | Unused | Pellets | 7 mm length | Full | 60% steam<br>Unsuccessful |
| 8 | Metal | Unused | Pellets | 10 mm length | Full | |
| 9 | Metal | Unused | Pellets | 10 mm length | 50% | |
| 10 | Metal | Activated | Pellets | 10 mm length | Full | 3 times |
| 11 | Metal | Activated | Pellets | 10 mm length | 50% | |

### 3.3.2 Gasification in the quartz glass reactor

The experiments in the quartz glass reactor were performed to gain familiarity with the system, especially with the steam generator, and learn how to fit the metal reactor into a system that was built for quartz glass reactors. These tests provided results to compare to those obtained from the metal reactor.

Two types of experiments were carried out in the quartz glass reactor. One full conversion with unused olivine as bed material, and one with activated olivine from the gasifier of the Chalmers power plant gasifier.

It was necessary to perform some tests of the fuel feeding system with different particle sizes, before starting the experiments with the quartz glass reactor, as there was no prior experience on the usage of different fuel particle sizes with the feeding system under the current conditions, i.e. with steam feed.

The char was added to the fuel feeding system before starting any gas flow. Otherwise even the small amount of gas that passes the hose clip would flush out some of the particles while adding them to the fuel feeding system.

The bed material was fluidized with the 500 mLn/min nitrogen during the heating. After reaching the operating temperature, the 400 mLn/min of $H_2O$ was added to the fluidizing gas. Then the 0.4 g of char was added via the fuel feeding system.

Two minutes after reaching maximum conversion, the experiments were stopped by turning off the steam supply of the entering gas so that only a nitrogen flow was sent to the reactor. The oven was also turned off to proceed to cooling down of the reactor. After 10-20 minutes the heating bands were turned off. It is necessary to heat the pipes after turning off the steam supply and to send some nitrogen to the reactor, otherwise the remaining steam could lead to condensed water in the pipes. The $N_2$

supply was turned off after 20-30 minutes. The bed material and the unconverted char were removed from the reactor once it reached room temperature.

### 3.3.3 Gasification inside a metal reactor

The char fuel used in the metal reactor was the same as that used in the quartz glass reactor, but the fuel particle size was larger in this case. All the successful experiments were made with three pieces of char pellet with a length of ~10 mm and a diameter of ~3 mm. Figure 9 shows an example of the feed char pellets.


*Figure 9: Char pellets used in the experiments with the metal reactor*

It was necessary to purge the fuel feeding system with $N_2$ and to heat insulate it, to avoid moisture or water condensation. For this reason, 100 mLn/min of $N_2$ was added to prevent the steam from condensation in the fuel feeding pipe. A second positive effect of purging the fuel feeding

line with $N_2$ was, that it was possible to flush out the air in the fuel feeding system while adding the fuel to the reactor.

Similarly to the experiments with the quartz reactor, the bed material was only fluidized with the 500 mLn/min of $N_2$ during the heat-up, while the steam was added once the temperature was reached. After reaching a stable flow, the air inside the fuel feeding system was flushed out with $N_2$ and the char was then added.

Five different types of experiments were carried out in the metal reactor.

1. Testing the compatibility of the fuel feeding system with different sizes of fuel
2. One full conversion with unused olivine as bed material
3. One 50% conversion with unused olivine as bed material
4. Three full conversions in a row with activated olivine as bed material
5. One 50% conversion with activated olivine as bed material

Experiment 1 was performed to find a char particle size which is feasible to feed and therefore enables repeatability of the experiments. They were performed with pellets of different sizes to obtain information about the possible problems with the fuel feeding system derived from the use of steam in the reactor, and also about the functionality of the fuel feeding system and its limitations in terms of the number and size of fuel particles.

The full conversion experiments (Experiments 2 and 4) were performed to compare the reaction rates of the different bed materials. Experiment 4 was performed to investigate the stability of the catalytic effect of the activated olivine and its performance after repeats without changing the bed material.

Experiments 3 and 5 were performed to generate samples of partly converted char in different bed materials for further analysis of the char particles by SEM/EDX.

## 3.4 DATA EVALUATION

The gasification process was evaluated by three different variables. As mentioned in Chapter 2.3 these variables are the instantaneous reaction rate *r*, the conversion rate $r_w$ and the degree of carbon conversion $X_C$ [22].

The conversion $X_C(t)$ at the time *t* is calculated as:

$$X_C(t) = \frac{m_c(t)}{m_{total}}$$

*Eq. 3-1*

Where $m_{total}$ is the weighed amount of char and $m_c(t)$ refers to the converted mass of carbon until it reaches the time *t* and it is calculated as

$$m_C(t) = \frac{pM_C}{RT}\int_0^t \dot{V}_{gas}(t)\left[x_{CO}(t) + x_{CO_2}(t) + x_{CH_4}(t)\right]dt \triangleq \frac{pM_c}{RT}\sum_{i=1}^{t}\dot{V}(i)$$

*Eq. 3-2*

$\dot{V}(i)$ is the gas flow of *CO*, $CO_2$ and $CH_4$ at the time interval *i* and is quantified as

$$\dot{V}(i) = \dot{V}_{gas}(i)\left[x_{CO}(i) + x_{CO_2}(i) + x_{CH_4}(i)\right]$$

*Eq. 3-3*

Where $x_{CO}(i)$, $x_{CO_2}(i)$ and , $x_{CH_4}(i)$ are the measured molar fraction at every time interval *i* of CO, $CO_2$ and $CH_4$, respectively.

The average conversion rate at each time *t*, $r_w(t)$ is calculated as:

$$r_w(t) = \frac{\dot{m}_c(t)}{m_{total}}$$

*Eq. 3-4*

where $\dot{m}_c(t)$ is the carbon mass flow at every time step *t* and it is calculated as,

$$\dot{m}_c(t) = \frac{pM_C}{RT} * \dot{V}_{gas}(t) * \left[x_{CO}(t) + x_{CO_2}(t) + x_{CH_4}(t)\right]$$

*Eq. 3-5*

The instantaneous reaction rate *r(t)* is calculated as

$$r(t) = \frac{r_w(t)}{1 - X}$$

*Eq. 3-6*

The volume percentage of $x_{CO}(i)$, $x_{CO_2}(i)$ and ,$x_{CH_4}(i)$ are measured every 1s. The total amount of char that was put inside the reactor, $m_{total}$ is defined as that before an experiment. With these four measurements and assuming that the gas flow in Eq. 3-2 can be described as the sum of areas under the function of an integral, it is possible to solve Eq. 3-1 to Eq. 3-6.

$M_C$ is defined as the molar mass of carbon, $p$ as the pressure at normal conditions, $T$ as the temperature at normal conditions, $x_i$ as the volume fraction of the component $i$ in the exhaust gas, $R$ as the ideal gas constant, $\dot{V}_{gas}(t)$ as the gas flow at time $t$, $\dot{m}_c(t)$ as the mass flow of carbon at $t$, and $m_c(t)$ as the overall converted carbon at $t$.

Table 10 shows the constants that were used in the calculation under normal conditions.

*Table 10: Constants for the calculations*

| | |
|---|---|
| $p$ | 101325 Pa |
| $T$ | 293.15 K |
| $M_C$ | 12.011 g*mol$^{-1}$ |
| $R$ | 8.314 J*mol$^{-1}$*K$^{-1}$ |

## 3.5 ANALYSIS OF THE CHAR

The char samples obtained in the experiments with the metal reactor were analysed with a scanning electron microscope method as well as with energy-dispersive X-ray spectroscopy (EDX).

### 3.5.1 Scanning electron microscope

To investigate the impact of different bed materials on the char surface, a Phenom Pro X scanning electron microscope (SEM) has been used. It was possible to look at the char particles with a light optical method with a 20 – 135x magnification as well as with an electron optical method with a 80 – 130000x magnification.

Besides magnifying the particles, it was also possible to carry out an EDX. This made it possible to obtain the exact composition of different parts of the char surface.

Three different char samples have been analysed. A reference char sample produced from devolatilization of the biomass fuel according to Chapter 3.2.1, a char sample after interrupting the steam gasification experiment after 50% conversion in a bed of unused olivine (Experiment 3), and one in a bed of active material (Experiment 5). Two or three different images (positions in the samples) were analysed for each char. Up to twelve different spots were analysed for each position. The elements analysed at each spot were Al, C, Ca, Cl, Fe, K, Mg, Mn, N, Na, Ni, O, P, S, and Si.

Three different distinct regions were observed in the char samples: salts, homogeneous and inhomogeneous areas of the char particle (please refer to Chapter 4.3). The spot analysis was categorized in these three regions.

# 4 RESULTS AND DISCUSSION

## 4.1 ASSESSMENT OF THE RIGHT PARTICLE SIZE FOR THE FUEL FEEDING SYSTEM

### Quartz glass reactor

Experiments have shown that it is not possible to feed the quartz glass reactor with whole char pellets without having some char blocked in the fuel feeding system. As mentioned in Chapter 3.2.1 the char pellets are too large for the pipes of the fuel feeding system.

Smaller particle sizes, between 125 µm and 180 µm got stuck due to the uneven surfaces and moisture or rather condensed water in the fuel feeding system. Beside these two effects, electrostatic forces and similar effects could have also caused problems while feeding.

Char that is stuck is a problem for the evaluation, because not all the fuel reaches the reaction zone. This leads to reduced repeatability and accuracy on the determination of char conversion. First, it is not possible to get information on how much char is fed to the reactor. Second, some char particles that got stuck in the feeding system could fall into the reactor at a later time and start to gasify. This leads to a biased result, because if all the char does not reach the reactor at the same time, the calculation has to be modified for each period of time where there was no addition of fuel. Another problem is, that it is not possible to get information on how much char fell into the reactor during the experiment and so the repeatability cannot be guaranteed.

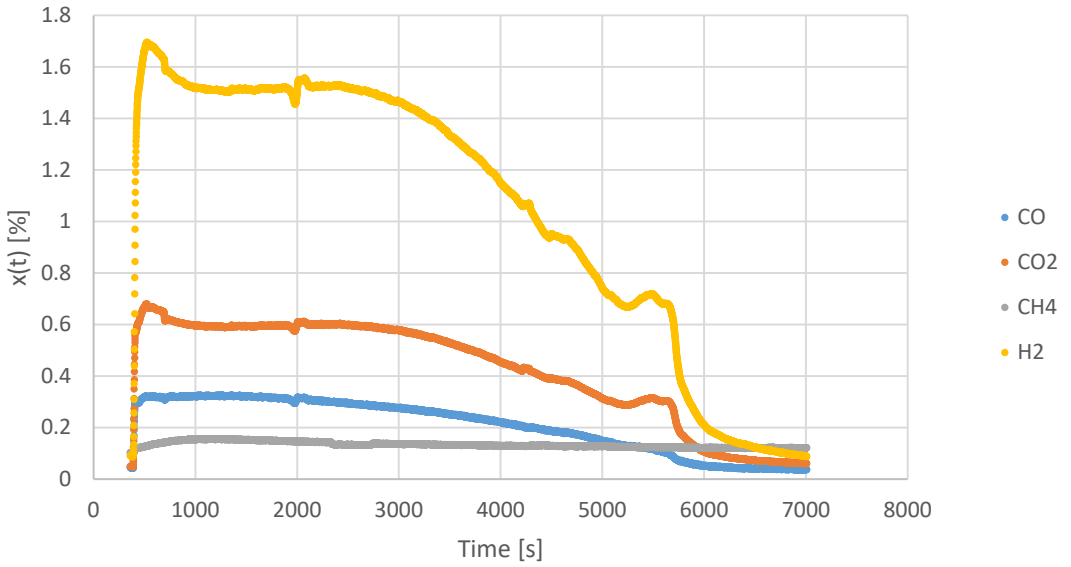


*Figure 10: Exhaust gas composition over time during an experiment with unused olivine as bed material and char particles with a size from 125 µm to 180 µm in the quartz glass reactor*

Figure 10 shows an experiment where some of the char particles got stuck in the fuel feeding system and as is clearly visible in the form of a peak at 2000 s and around 5500 s, some of the stuck particles fell into the reactor while some of the char was already gasified.

Particle sizes between 500 µm and 710 µm have proven to work well with the fuel feeding system of the quartz glass reactor. Possibly nearly all the char within this size range reaches the fluidized bed and provides repeatable experiments.

### Metal reactor

Different pellet sizes have been investigated in experiments. Trials with pellets of a length of 6-7 mm have shown, that char with a length smaller than the inner diameter of the pipe could be problematic. During most of the trials with the smaller ones, the pellets blocked each other so that only two fell into the reactor or that some reached the reactor after the first pellets were already gasified for some seconds. This effect was even stronger when using 60% steam in the fluidizing gas instead of 44.4%.

With 60% steam not even one of the smaller pellets fell into the reactor. The main reason for this was the moisture inside the fuel feeding system. It was found that large char particle sizes are well-suited to the fuel feeding system of the metal reactor. The char pellets which did not cause any practical problem in this reactor had a length of 10 mm and a diameter of 7 mm as shown in Figure 9 of Chapter 3.2.2.

## 4.2 FULL CHAR CONVERSION EXPERIMENTS

Experiments with the unused olivine and the activated olivine in the quartz glass reactor have shown a significant difference between the reaction rates during the char gasification. Figure 11 and Figure 12 show that the reaction of the experiment with activated olivine was two times faster than when using a bed of unused olivine.

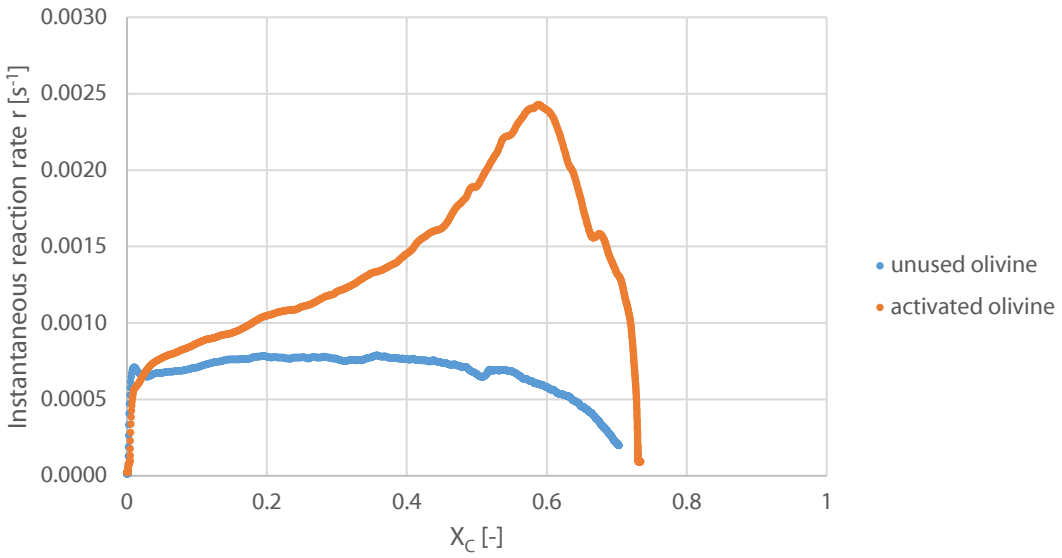


*Figure 11: Instantaneous reaction rate (r) of char gasification as a function of the degree of conversion ($X_C$). Experiments in the quartz glass reactor with 44.4% of steam in $N_2$ and char particle sizes of 500 µm - 710 µm. Bed temperature 900 °C.*

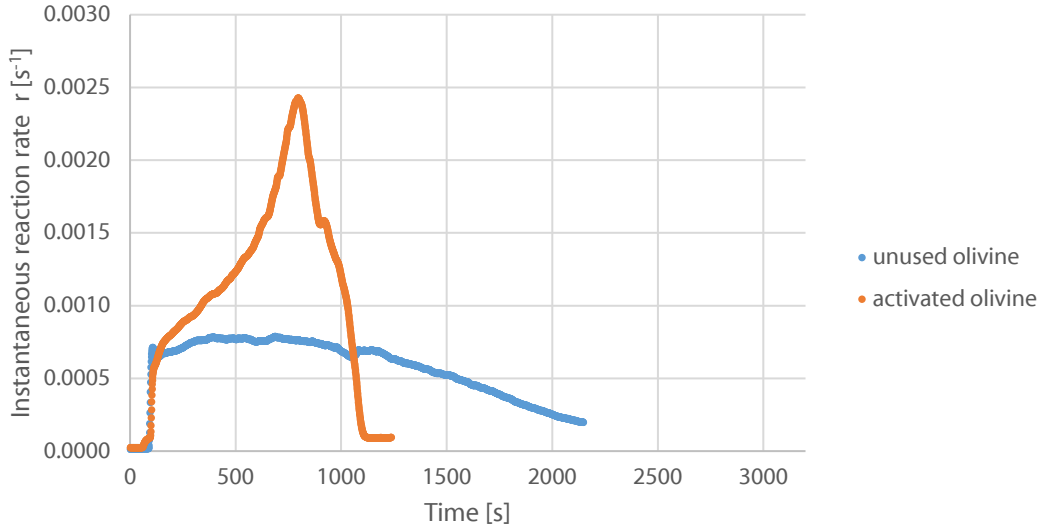


*Figure 12: Instantaneous reaction rate (r) of char gasification as a function of time. Experiments in the quartz glass reactor with 44.4% of steam in $N_2$ and char particle sizes of 500 µm - 710 µm. Bed temperature 900 °C.*

This effect was also observed during the experiments with unused olivine and activated olivine in the metal reactor. Figure 13 and Figure 14 show the same effect as was seen in the quartz glass reactor.

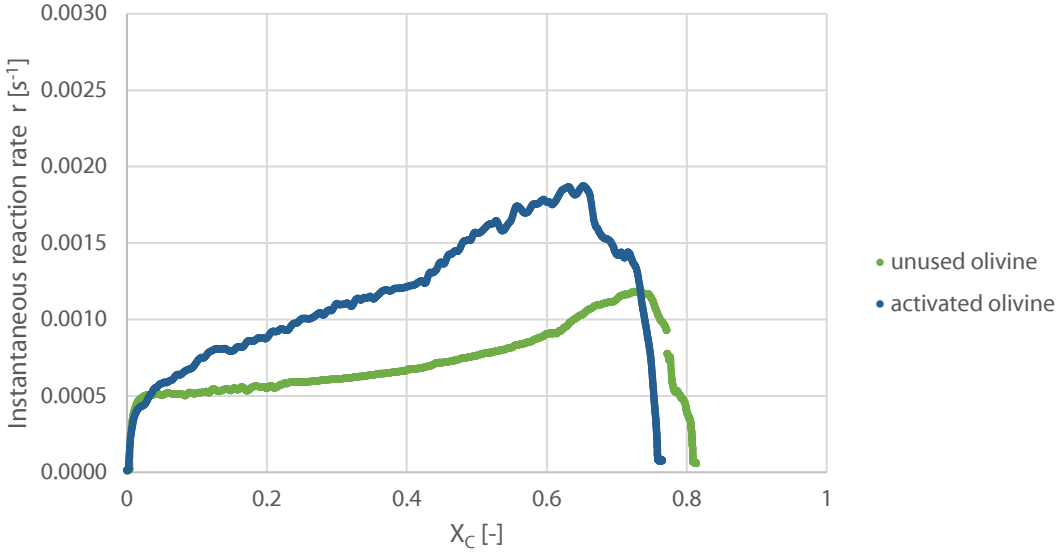


*Figure 13: Instantaneous reaction rate (r) of char gasification as a function of the degree of conversion ($X_C$). Experiments in the metal reactor with 44.4% of steam in $N_2$ and char particle size 10 mm x 7 mm. Bed temperature 900 °C.*

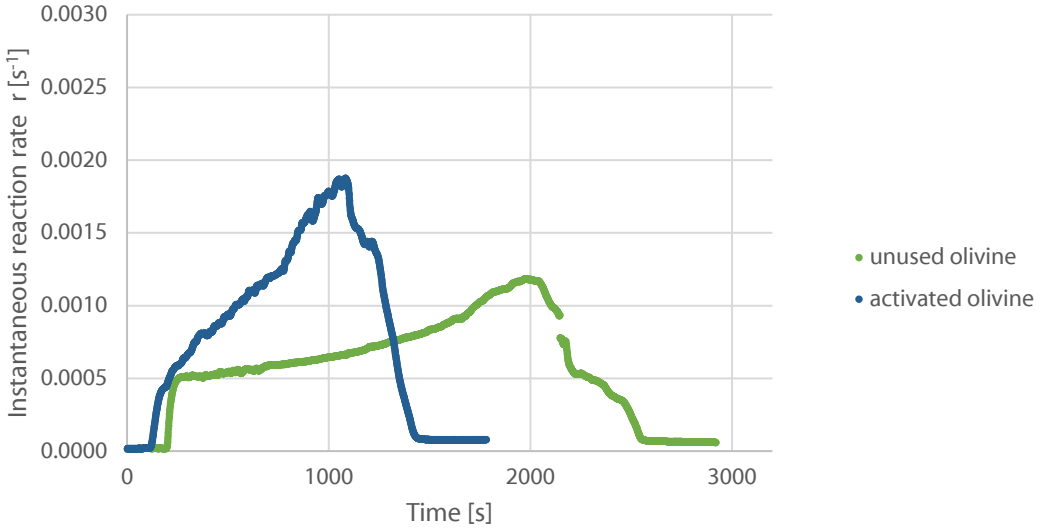


*Figure 14: Instantaneous reaction rate (r) of char gasification as a function of time. Experiments in the metal reactor with 44.4% of steam in $N_2$ and char particle size of 10 mm x 7 mm. Bed temperature 900 °C.*

This positive effect of the activated olivine on the gasification reaction can be caused by the presence of alkali metals inside the bed material, as the olivine was activated by adding potassium salts to the bed in the Chalmers gasifier. As described in Chapter 2.4 potassium has been investigated by other researchers for its catalytic activity on the steam gasification of char.

The trends in both reactors are similar, but the overall reaction rates in the metal reactor are 20% lower than in the quartz glass reactor. The reason for the different reaction rates between the two reactors even with the same bed material can be attributed to the smaller particle sizes that are used in the quartz glass reactor experiments. A higher specific particle size of the char, could cause more interaction between the catalytic material in the bed material and the char surface. This could also explain why $r$ stays stable during experiments with unused olivine as bed material but behaves unstable with active material. Another possible explanation contributing to the lower rate of char gasification in the metal reactor is the lower fluidization in the metal reactor. The velocity in the quartz glass reactor is $U_Q$ = 0.142 m/s while the velocity in the metal reactor is $U_M$ = 0.042 m/s, as a result of the two times bigger diameter of the metal

reactor. A higher fluidization could also increase the possible interaction between the catalytic material and the char, based on a higher amount of mixing of the bed material.

Comparing Figure 11 and Figure 12 with Figure 13 and Figure 14 shows that the instantaneous reaction rate in the unused olivine experiment in the quartz glass reactor is all the time decreasing, while the one performed in the metal reactor is increasing up to a maximum before the conversion stops. This could be due to the differences in reactor size, reactor material, or the differences in experimental conditions, such as particle size and fluidization velocity.

It was observed that in all experiments the char conversion did not reach 100%. Several things can explain this. One reason is, that due to moisture, condensed water, and uneven surfaces of the fuel feeding system, it is not possible to feed the reactor with all the char that was weighed. This effect gains more importance when it comes to experiments in the quartz glass reactor as the fuel particles were smaller and more difficult to feed. As mentioned in Chapter 4.1 the fuel feeding system caused the biggest difficulties during the experiments with the quartz glass reactor.

The main reason seems to be that the char does not consist solely of carbon. Fresh char also contains ash, moisture, oxygen, hydrogen and nitrogen. Furthermore, there might be possible errors in the measurement and in the calibration of the measurement tools. The expected conversion for the experiments in the metal reactor is therefore around 80%, and for the ones in the quartz glass reactor it is even lower.

### 4.2.1 Gasification with activated olivine as bed material

As mentioned in Chapter 2.5 the alkali metals which are in the activated olivine can have a catalytic effect on the gasification. However, the catalytic activity of olivine on the char gasification seems to decrease over time. The three consecutive conversion experiments with the activated

olivine as bed material have shown an interesting behaviour. After each experiment, the conversion rate decreased by 33% and the necessary time for the full char conversion had increased by 20%. Figure 15 and Figure 16 show the phenomenon of the decreasing conversion rate.

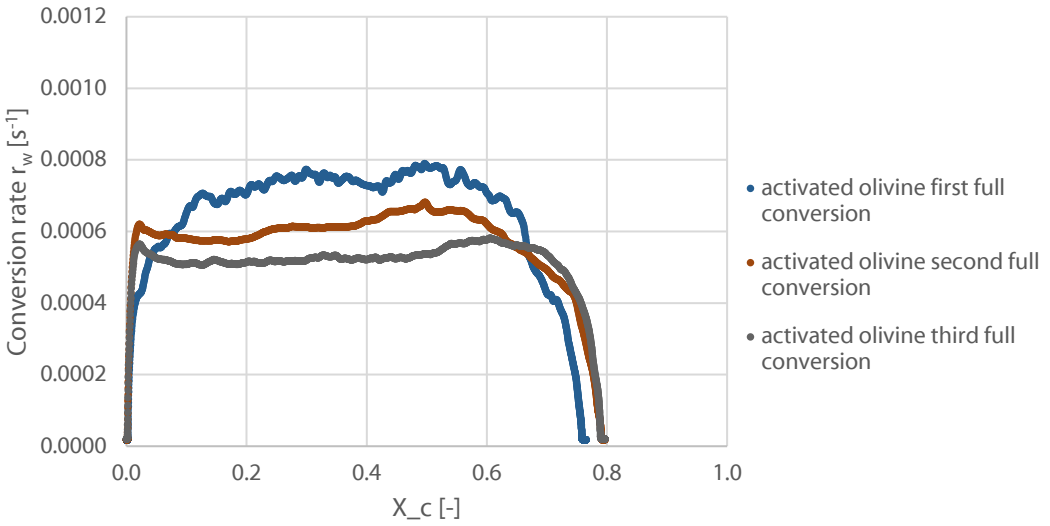


*Figure 15: Conversion rate ($r_w$) of char gasification as a function of the degree of conversion ($X_C$). Experiments in the metal reactor with 44.4% of steam in $N_2$ and char particle size 10 mm x 7 mm. Bed temperature 900 °C.*

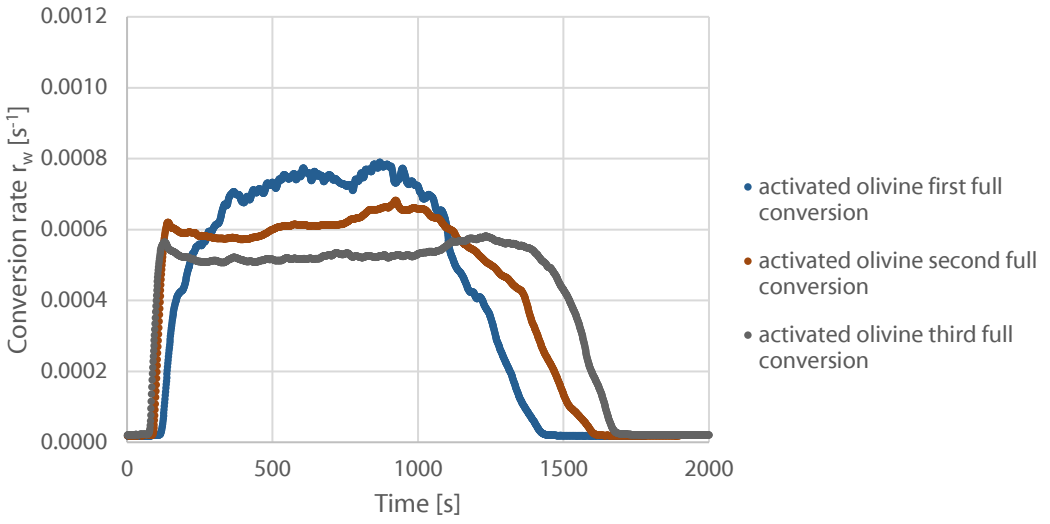


*Figure 16: Conversion rate ($r_w$) of char gasification as a function of time. Experiments in the metal reactor with 44.4% of steam in $N_2$ and char particle size 10 mm x 7 mm. Bed temperature 900 °C.*

This effect could be explained by side reactions (cf. Eq. 2-8 to Eq. 2-11 of Chapter 2.4.1) which consumed the catalytic material. This would imply that after each full conversion experiment with the same bed material, the amount of available potassium in the activated olivine is possibly decreasing. This decrease leads to a smaller catalytic effect of the bed material on the gasification reaction which results in a lower conversion rate and a greater need of time for a full conversion. Another reason for a possible decrease is the high volatility of some K-salts like KOH, which could lead to potassium being flushed out of the system with the exhaust gas.

## 4.3 ANALYSIS OF PARTLY GASIFIED CHAR

SEM analysis of the char has revealed three distinct areas in the surface of the char. Figure 17 shows the surface of char after a 50% conversion experiment with active olivine as bed material. The numbers from 1 to 3 show the distinct areas of the char: inhomogeneous area (1), homogeneous area (2), and salts (3). 10 sites in this image were analysed by EDX, covering the three differentiated areas.

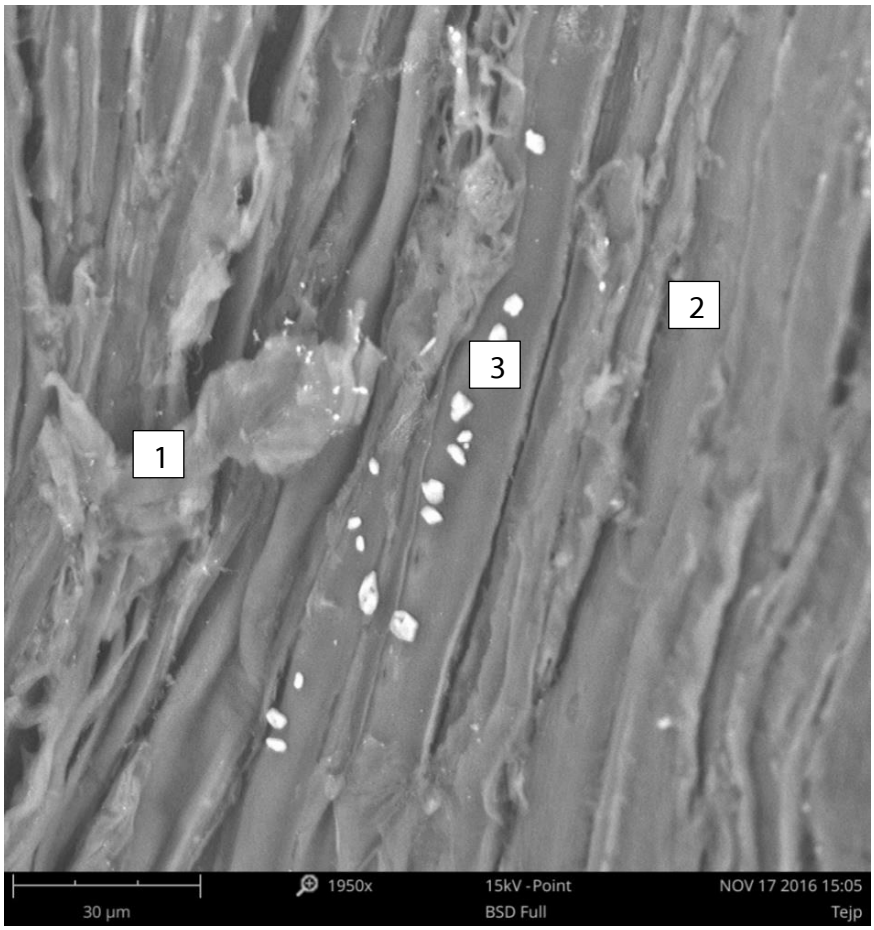


*Figure 17: Char at 50% conversion by steam gasification in a bed of active olivine. The three distinct areas: inhomogeneous area (1), homogeneous area (2), and salts (3).*

Ten SEM images were taken and have been analysed with EDX:

- 3 images of fresh char
- 3 images of char at 50% conversion by steam gasification in a bed of unused olivine
- 4 images of char at 50% conversion by steam gasification in a bed of active olivine

The analysis of the homogeneous and inhomogeneous areas of the char surface has uncovered no significant difference. It has also shown that the major elements are C and O. Figure 18 displays the minor components of the inhomogeneous and homogeneous areas of the char surface.

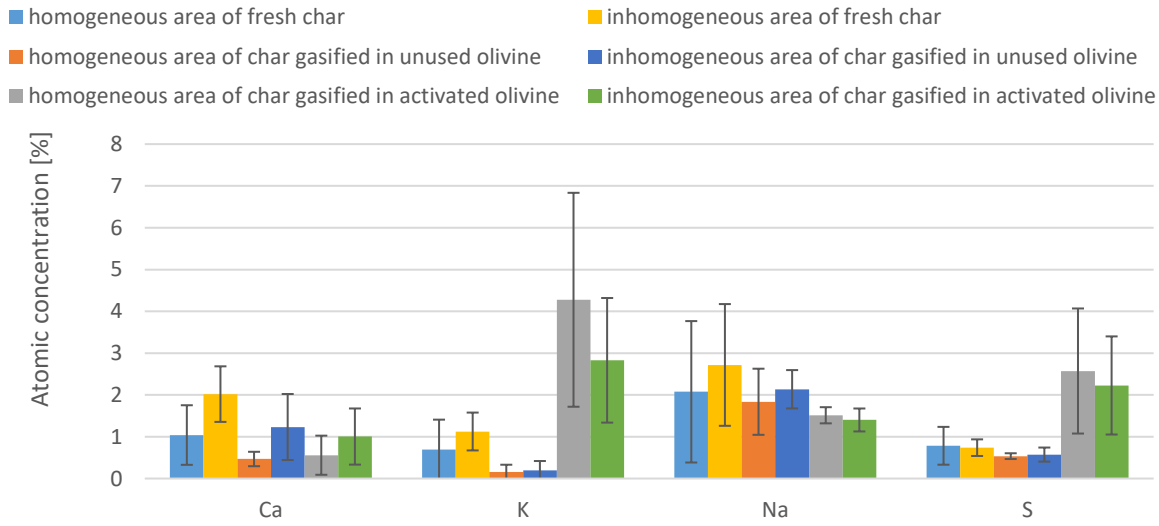


*Figure 18: Composition of the minor components of the inhomogeneous and homogeneous areas of the char surface. Char particles at 50% conversion. Only elements with an atomic concentration of >1% are shown.*

Fresh char, and char that had been partly gasified in unused olivine, and char that had been partly gasified in used olivine, were all three respectively, analysed with EDX in a SEM for their composition. All three char sample type compositions formed mutual overlap within the ranges defined by their standard deviations, meaning that their compositions were comparable. The biggest differences correspond to S and K. The SEM/EDX analysis of fresh char and of the char at 50% conversion in a bed

of activated olivine have shown that S and K have increased from <1% up to 2.5% of S and 4.2% of K. This increase follows from gasification in the activated bed material, which contains both elements due to the activation process. The increase of S and K means that the gasification process of char in the activated bed material leads to active components in the char matrix.

The images have shown salts ranging between 1 µm and 10 µm. They are visible because of their shape and their brightness on SEM images. The increase of K after gasification in activated olivine is even higher in the salts analysis. Table 11 shows the EDX analysis of the salts found in the different char samples. The samples of fresh char and char gasified in a bed of unused olivine only showed salts containing Fe and Ca. The EDX of the char gasified in a bed of activated olivine has salts containing K, Si and Ca. The appearance of K salts is caused by the $K_2CO_3$ which is part of the activated olivine. The K salts on the char surface could be a result of crystallization during the cooldown.

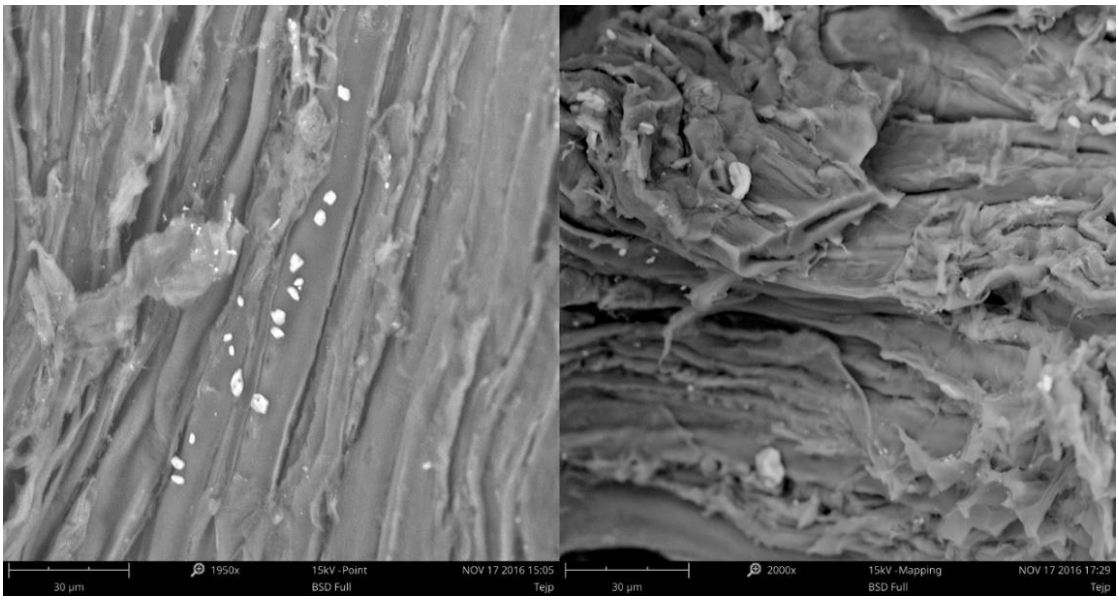


*Figure 19: Char at 50% conversion by steam gasification in bed of active olivine with K salts.*

*Table 11: Average composition of the salts shown in Figure 20. Contains only elements above 1% atomic concentration.*

| | Atomic concentration [%] | Deviation |
|---|---|---|
| **O** | 54.70 | 12.71 |
| **C** | 16.17 | 4.87 |
| **K** | 15.41 | 11.18 |
| **N** | 9.32 | 0.99 |

Figure 19 shows the areas with potassium salts and Table 11 the composition of the salt elements with an atomic concentration >1%. Table 11 shows a high standard deviation for K in the sample char at 50% conversion by steam gasification in bed of active olivine. The high standard deviation of K resulted from one EDX analysed site which gave an unusually high reading for the concentration of K of 39.6%. While all K salts except for this aberration have shown a K concentration of 8.2% to 14.8%. This leads to a standard deviation of ±11.2, which refers to a deviation of ~73%.

A stoichiometric analysis follows that the K salts with 8.2% to 14.8% K are most likely $K_2CO_3$ with 33% of C as part of the salt and the rest as inclusions in the salts or carbon residues on the surface of the salts. From this, the stoichiometric analysis of the aberration shows that it consists of two salts, 75% $K_2O$ and 25% $K_2CO_3$. Some salts, while they were visible on the char surface, were outside of the focus range of the instrument and therefore appeared blurry. And so another possible reason considered for the high amount of K, could potentially be a reduced measurement accuracy resulting from some salts being outside the focus range.

The average K concentration of the salts without the aberration would be 10.5% with a standard deviation of ±2.5. Table 12 shows the average composition of the salts with and without the aberration on the surface of the char at 50% conversion by steam gasification.

*Table 12: Salt composition of activated olivine gasified char - with and without aberration*

| | Without aberration | | With aberration | | | Without aberration | | With aberration | |
|---|---|---|---|---|---|---|---|---|---|
| | Conc. [%] | Deviation | Conc. [%] | Deviation | | Conc. [%] | Deviation | Conc. [%] | Deviation |
| **O** | 58.81 | 5.95 | 54.70 | 12.71 | **Al** | 0.43 | 0.02 | 0.41 | 0.06 |
| **C** | 17.29 | 5.32 | 16.17 | 4.87 | **Si** | 0.39 | 0.04 | 0.37 | 0.05 |
| **K** | 10.51 | 2.53 | 15.41 | 11.18 | **P** | 0.23 | 0.05 | 0.25 | 0.05 |
| **N** | 9.02 | 0.51 | 9.32 | 0.99 | **Cl** | 0.19 | 0.05 | 0.23 | 0.11 |
| **Na** | 1.04 | 0.26 | 0.95 | 0.26 | **Ni** | 0.11 | 0.08 | 0.10 | 0.09 |
| **S** | 0.85 | 0.27 | 0.89 | 0.24 | **Fe** | 0.06 | 0.05 | 0.05 | 0.05 |
| **Mg** | 0.79 | 0.15 | 0.71 | 0.18 | **Mn** | 0.05 | 0.04 | 0.04 | 0.04 |
| **Ca** | 0.25 | 0.12 | 0.42 | 0.37 | | | | | |

Figure 20 shows a salt containing Si, Ca, K and Al (left) and Ca salts (right). Two sites on the salt shown on the left side of Figure 20 have been analysed. The analysis shows a higher amount of Si, K and Al salts than in the fresh char. The increase of these three elements can be explained by the remaining ash that contains all three elements. However, the K increase is unproportionally high compared to the other elements, this can be explained by the activated bed material as mentioned above.

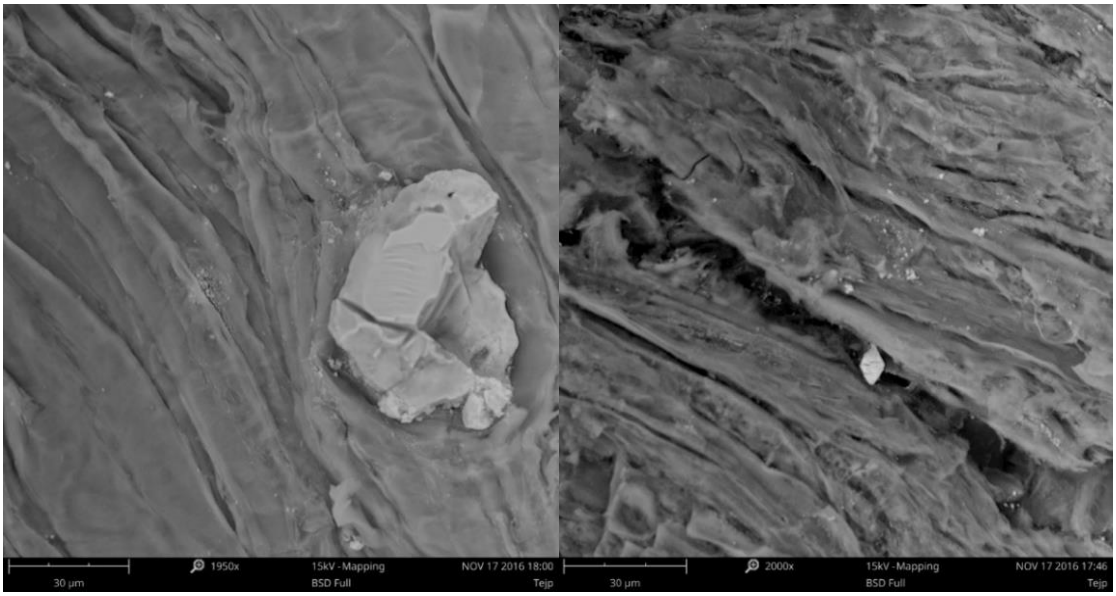


*Figure 20: Left: Si and Ca salts at the surface of the char gasified in activated olivine. Right: Ca salt on the surface of the char gasified in activated olivine.*

# 5 CONCLUSION AND FUTURE WORK PERSPECTIVE

The main questions of this master thesis were:

- *Which effects on the gasification process can be investigated when using activated and unused olivine as bed material?*
- *What can cause the effects of the two bed materials on the gasification process?*
- *What impact can alkali metals have on the gasification process?*

To answer these hypotheses, a brand new setup with a metal reactor was built as an alternative to quartz glass. Consequently it was necessary to define a new experimental procedure and to devise a method of evaluation of the measured data.

It was possible to find good operating conditions for the metal reactor during the first tests with the new setup. The tests have shown that the new setup requires more preparation time, but that it also works more reliably with a steam environment.

The char gasification experiments have shown significant differences between the reactivity of the char in a bed of unused olivine as compared to a similar case in a bed of activated olivine. This verifies a catalytic effect on the steam gasification reaction which is attributed to the activated olivine. The catalytic effect of the activated bed material results in a 50% reduction of the time to reach full conversion, as compared to the time that is necessary for full conversion in a bed of unused olivine.

It was found that the catalytic effect of the activated olivine in the steam gasification reaction was decreasing over time. To gather information about this behaviour, it would be necessary to measure the alkali content

of the exhaust gas. This could clarify if the reducing catalytic effect occurs because alkali metals are leaving the reactor with the exhaust gas.

To find visible differences between the fresh char and the gasified char samples, the char samples were analysed with a SEM and EDX. The analysis has shown that the surface composition of fresh char, and of char that was gasified in unused olivine was nearly the same. The surface analysis of the char that was gasified in activated olivine was found to contain potassium and sulfur on all analysed sites of the char matrix, while the fresh char was not. This leads to the hypothesis that some of the potassium was transferred from the activated olivine to the char matrix during the gasification process.

Another difference between the char gasified in a bed of active olivine and that in a bed of unused olivine, was that for the one of active olivine, there were potassium salts that crystallised on the surface of the char. These salts were not observable on the fresh char nor on the char gasified in unused olivine. This shows that the char was in contact with salts during the gasification process in activated olivine. Other than the potassium salts, it was also possible to find other salts such as calcium, but these salts were also observable in the fresh char, which means that they were part of the char from the beginning.

Further research work could focus on the transfer of catalytic material to the char matrix, or investigate if there is more catalytic activity in the gas phase or in the solid phase.

# BIBLIOGRAPHY


[1] M. I. Hoffert, K. Caldeira, A. K. Jain, E. F. Haites, L. D. Harvey, S. D. Potter, M. E. Schlesinger, S. H. Schneider, R. G. Watts, T. M. Wigley and D. J. Wuebbles, "Energy implications of future stabilization of atmospheric CO2 content," *Nature,* vol. 395, pp. 881-884, 1998.

[2] G. Berndes, M. Hoogwijk and R. van den Broek, "The contribution of biomass in the future global energy supply: a review of 17 studies," *Biomass and Bioenergy,* vol. 25, pp. 1-28, 2003.

[3] M. Kaltschmitt, H. Hartmann and H. Hofbauer, Energie aus Biomasse, Berlin Heidelberg: Springer-Verlag, 2009.

[4] F. u. W. Bundesministerium für Wissenschaft, "Energiestatus Österreich 2015," Bundesministerium für Wissenschaft, Forschung und Wirtschaft, Vienna, 2015.

[5] D. O. Hall and J. I. Scrase, "Will biomass be the environmentally friendly fuel of the future?," *Biomass and Bioenergy,* vol. 15, no. 4-5, pp. 357-367, 1998.

[6] J. Marinkovic, Choice of bed material: a critical parameter in the optimization of dual fluidized bed systems, Gothenburg: PhD thesis, 2016, pp. 5-11.

[7] J. C. Schmid, S. Müller and H. Hofbauer, "Eine neue Generation der DUAL FLUID Dampfvergasung als Versuchsanlage an der TU Wien," Vienna, 2014.

[8] J. Fuchs, J. C. Schmid and H. Hofbauer, "Kaltmodelluntersuchungen zu einer innovativen Zweibettwirbelschicht," Leoben, 2013.

[9] P. Basu, COMBUSTION and GASIFICATION in FLUIDIZED BEDS, Halifax: Taylor & Francis Group, 2006, p. 21.

[10] C. Wen and Y. Yu, "A generalized method for predicting the minimum fluidization velocity," *AIChE Journal,* vol. 12, no. 3, pp. 610-612, 1966.

[11] W. R. Gossens, "Classification of fluidized particles by Archimedes number," *Powder Technology,* vol. 98, no. 1, pp. 48-53, 1998.

[12] P. B. Kowalczuk and J. Drzymala, "Physical meaning of the Sauter mean diameter of spherical particulate matter," *Particulate Science and Technology,* pp. 1-3, 2015.

[13] D. Kunii and O. Levenspiel, Fluidization Engineering, Stoneham: Butterworth-Heinemann, 1991, pp. 68-76.

[14] R. S. Subramanian, "Clarkson University Homepage," 02 2007. [Online]. Available: http://web2.clarkson.edu/projects/subramanian/ch301/notes/packfluidbed.pdf. [Accessed 22 11 2016].

[15] D. Geldart, "Types of Gas Fluidization," *Powder Technology,* vol. 7, pp. 285-292, 1973.

[16] H. B. Goyal, D. Seal and R. C. Saxena, "Bio-fuels from thermochemical conversion renewable resources: A review," *Renewable and Sustainable Energy Reviews,* vol. 12, no. 2, pp. 504-517, 2008.

[17] S. Zafar, "ALTENERGYMAG," LJB MANAGEMENT INC., 01 02 2009. [Online]. Available: http://www.altenergymag.com/content.php?issue_number=09.02.01&article=pyrolysis. [Accessed 15 11 2016].

[18] D. Meier, J. Welling and B. Wosnitza, "Pyrolyse," in *Energie aus Biomasse*, M. Kaltschmitt, H. Hartmann and H. Hofbauer, Eds., Heidelberg, Springer-Verlag Berlin Heidelberg, 2009, pp. 671-710.

[19] P.-E. Bengtsson, "Introduction to Thermodynamics and Chemistry in Combustion," in *COMBUSTION ENGINEERING*, H. Thunman, Ed., Gothenburg, Lecture Book, 2013, p. 3.1.

[20] T. Nussbaumer, H. Hartmann, H. Hofbauer and J. Good, "Direkte thermo-chemische Umwandlung (Verbrennung)," in *Energie aus Biomasse*, M. Kaltschmitt, H. Hartmann and H. Hofbauer, Eds., Heidelberg, Springer-Verlag Berlin Heidelberg, 2009, pp. 463-598.

[21] A. Khan, W. d. Jong, P. Jansens and H. Spliethoff, "Biomass combustion in fluidized bed boilers: Potential problems and remedies," *Fuel Processing Technology,* vol. 90, no. 1, pp. 21-50, 2009.

[22] M. Keller, H. Leion, T. Mattisson and A. Lyngfelt, "Gasification inhibition in chemical-looping combustion with solid fuels," *Combustion and Flame,* vol. 158, pp. 395-396, 2011.

[23] D. Sutton, B. Kelleher and J. R. Ross, "Review of literature on catalysts for biomass gasification," *Fuel Processing Technology,* vol. 73, no. 3, pp. 155-173, 2001.

[24] M. Barrio, B. Gøbel, H. Risnes, U. B. Henriksen, J. E. Hustad and L. H. Sørensen, "Steam gasification of wood char and the effect of hydrogen inhibition on the chemical kinetics," in *Progress in Thermochemical Biomass Conversion*, Oxford, Blackwell Science Ltd, 2000.

[25] J. Wang, M. Jiang, Y. Yihong, Z. Yanmei and C. Jianqin, "Steam gasification of coal char catalyzed by K2CO3 for enhanced production of hydrogen without formation of methane," *Fuel,* vol. 88, pp. 1572-1579, 2009.

[26] C. Dupont, G. Boissonnet, J.-M. Seiler, P. Gauthier and D. Schweich, "Study about the kinetic processes of biomass steam gasification," *Fuel,* vol. 86, pp. 32-40, 2007.

[27] S. Koppatz, C. Pfeifer and H. Hofbauer, "Comparison of the performance behaviour of silica sand and olivine in a dual fluidised bed reactor system for steam gasification of biomass at pilot plant scale," *Chemical Engineering Journal,* vol. 175, pp. 468-483, 2011.

[28] C. Pfeifer, R. Rauch and H. Hofbauer, "In-Bed Catalytic Tar Reduction in a Dual Fluidized Bed Biomass Steam Gasifier," *Industrial & Engineering Chemistry Research,* vol. 43, no. 7, pp. 1634-1640, 2004.

[29] J. Marinkovic, H. Thunman, P. Knutsson and M. Seemann, "Characteristics of olivine as a bed material in an indirect biomass

gasifier," *Chemical Engineering Journal,* vol. 279, pp. 555-566, 2015.

[30] C. H. Bartholomew, "Mechanisms of catalyst deactivation," *Applied Catalysis A: General,* vol. 212, no. 1-2, pp. 17-60, 2001.

[31] J. Gil, M. A. Caballero, J. A. Martín, M.-P. Aznar and J. Corella, "Biomass Gasification with Air in a Fluidized Bed: Effect of the In-Bed Use of Dolomite under Different Operation Conditions," *Industrial & Engineering Chemistry Research,* vol. 38, no. 11, pp. 4226-5235, 1999.

[32] T. B. Vilches, J. Marinkovic, M. Seemann and H. Thunman, "Comparing Active Bed Materials in a Dual Fluidized Bed Biomass Gasifier: Olivine, Bauxite, Quartz-Sand, and Ilmenite," *energy & fuels,* vol. 30, pp. 4848-4857, 2016.

[33] F. Kirnbauer, V. Wilk, H. Kitzler, S. Kern and H. Hofbauer, "The positive effects of bed material coating on tar reduction in a dual fluidized bed gasifier," *Fuel,* vol. 95, pp. 553-562, 2012.

[34] S. Rapagnà, N. Jand, A. Kiennemann and P. U. Foscolo, "Steam-gasification of biomass in a fluidised-bed of olivine particles," *Biomass and Bioenergy,* vol. 19, no. 3, pp. 187-197, 2000.

[35] D. W. McKee, "Mechanisms of alkali metal catalysed gasification of carbon," *Fuel,* vol. 62, no. 2, pp. 170-175, 1983.

[36] G. L. Guzman and E. E. Wolf, "Kinetics of K2CO3-Catalyzed steam gasification of Carbon and Coal," *Ind. Eng. Chem. Process. Des. Dev.,* vol. 21, pp. 25-29, 1982.

[37] A. M. Radwan, "An overview on gasification of biomass for production of hydrogen rich gas," *Der Chemica Sinica,* vol. 3, pp. 323-335, 2012.

[38] G. Lagaly, W. Tufar, A. Minihan and A. Lovell, "Alkali Silicates," in *Ullmann's Encyclopedia of Industrial Chemistry*, Wiley-VCH, 2000.

[39] R. R. Brown and K. O. Bennington, "Thermodynamic properties of potassium metasilicate (K2SiO3)," *Thermochimica Acta,* vol. 122, pp. 289-294, 1987.

[40] T. B. Vilches and H. Thunman, "Impact of oxygen transport on char conversion in dual fluidized bed systems," *Nordic Flame Days Copenhagen,* 2015.

# LIST OF FIGURES

# LIST OF TABLES

# APPENDIX A

**Salt**

| | Fresh char | | Char gasified in unused olivine | | Char gasified in active olivine | |
|---|---|---|---|---|---|---|
| | Atomic conc. [%] | Standard deviation | Atomic conc. [%] | Standard deviation | Atomic conc. [%] | Standard deviation |
| Al | 1.33 | 0.64 | 0.76 | 0.10 | 0.41 | 0.06 |
| C | 29.29 | 12.33 | 20.39 | 7.08 | 16.17 | 4.87 |
| Ca | 11.63 | 12.18 | 6.96 | 5.08 | 0.42 | 0.37 |
| Cl | 0.80 | 0.61 | 0.44 | 0.06 | 0.23 | 0.11 |
| Fe | 5.66 | 9.02 | 0.45 | 0.31 | 0.05 | 0.05 |
| K | 0.94 | 0.82 | 0.00 | 0.00 | 15.41 | 11.18 |
| Mg | 2.10 | 1.05 | 1.97 | 0.37 | 0.71 | 0.18 |
| Mn | 1.06 | 1.13 | 0.51 | 0.33 | 0.04 | 0.04 |
| N | 9.61 | 5.02 | 14.03 | 1.61 | 9.32 | 0.99 |
| Na | 2.56 | 2.04 | 2.11 | 0.28 | 0.95 | 0.26 |
| Ni | 0.73 | 1.73 | 0.07 | 0.22 | 0.10 | 0.09 |
| O | 29.32 | 11.83 | 50.35 | 7.80 | 54.70 | 12.71 |
| P | 1.29 | 1.20 | 0.68 | 0.08 | 0.25 | 0.05 |
| S | 0.77 | 0.48 | 0.51 | 0.14 | 0.89 | 0.24 |
| Si | 2.91 | 3.89 | 0.77 | 0.16 | 0.37 | 0.05 |

**Homogeneous area**

| | Fresh char | | Char gasified in unused olivine | | Char gasified in active olivine | |
|---|---|---|---|---|---|---|
| | Atomic conc. [%] | Standard deviation | Atomic conc. [%] | Standard deviation | Atomic conc. [%] | Standard deviation |
| Al | 0.99 | 0.58 | 0.81 | 0.18 | 0.61 | 0.11 |
| C | 52.22 | 12.88 | 53.89 | 2.82 | 51.36 | 4.54 |
| Ca | 1.04 | 0.71 | 0.47 | 0.17 | 0.56 | 0.47 |
| Cl | 0.70 | 0.53 | 0.47 | 0.17 | 0.53 | 0.32 |
| Fe | 0.46 | 1.01 | 0.07 | 0.20 | 0.11 | 0.10 |
| K | 0.69 | 0.72 | 0.16 | 0.17 | 4.28 | 2.56 |
| Mg | 1.34 | 0.83 | 1.51 | 0.34 | 1.21 | 0.18 |
| Mn | 0.41 | 0.69 | 0.08 | 0.24 | 0.14 | 0.12 |
| N | 10.49 | 3.87 | 14.17 | 2.13 | 13.74 | 0.93 |
| Na | 2.08 | 1.69 | 1.84 | 0.79 | 1.51 | 0.19 |
| Ni | 0.33 | 0.64 | 0.12 | 0.35 | 0.05 | 0.09 |
| O | 26.98 | 7.41 | 24.56 | 3.50 | 38.79 | 3.55 |
| P | 0.71 | 0.40 | 0.66 | 0.15 | 0.51 | 0.27 |
| S | 0.78 | 0.45 | 0.54 | 0.07 | 2.57 | 1.50 |
| Si | 0.78 | 0.40 | 0.66 | 0.21 | 0.69 | 0.18 |

| | Inhomogeneous area | | | | | |
|---|---|---|---|---|---|---|
| | Fresh char | | Char gasified in unused olivine | | Char gasified in active olivine | |
| | Atomic conc. [%] | Standard deviation | Atomic conc. [%] | Standard deviation | Atomic conc. [%] | Standard deviation |
| Al | 1.16 | 0.52 | 0.90 | 0.11 | 0.53 | 0.11 |
| C | 42.71 | 9.02 | 46.27 | 6.33 | 40.62 | 2.37 |
| Ca | 2.02 | 0.66 | 1.23 | 0.79 | 1.01 | 0.67 |
| Cl | 0.71 | 0.37 | 0.48 | 0.09 | 0.60 | 0.37 |
| Fe | 0.24 | 0.52 | 0.17 | 0.23 | 0.11 | 0.08 |
| K | 1.13 | 0.45 | 0.19 | 0.23 | 2.83 | 1.49 |
| Mg | 1.60 | 0.81 | 1.65 | 0.22 | 1.28 | 0.23 |
| Mn | 0.46 | 0.80 | 0.29 | 0.25 | 0.13 | 0.11 |
| N | 10.79 | 3.17 | 12.97 | 1.35 | 11.67 | 0.78 |
| Na | 2.72 | 1.46 | 2.14 | 0.46 | 1.40 | 0.27 |
| Ni | 0.50 | 0.50 | 0.17 | 0.22 | 0.04 | 0.10 |
| O | 33.67 | 5.09 | 31.48 | 4.88 | 36.48 | 3.34 |
| P | 0.81 | 0.21 | 0.78 | 0.29 | 0.48 | 0.17 |
| S | 0.74 | 0.20 | 0.57 | 0.17 | 2.23 | 1.17 |
| Si | 0.76 | 0.20 | 0.70 | 0.17 | 0.61 | 0.18 |

# APPENDIX B

## Calculation $U_{mf}$:

$X_{N_2} = 0.56$ $X_{H_2O} = 0.44$

$\mu_{N_2}(900°C) = 46.2 * 10^{-6} Pa\ s$ $\mu_{H_2O}(900°C) = 44 * 10^{-6} Pa\ s$

$M_{N_2} = 28 \frac{g}{mol}$ $M_{H_2O} = 18 \frac{g}{mol}$

$$\Phi_{N_2,H_2O} = \frac{1}{2\sqrt{2}} * \left(1 + \frac{M_{N_2}}{M_{H_2O}}\right)^{-\frac{1}{2}} * \left[1 + \left(\frac{\mu_{N_2}(900°C)}{\mu_{H_2O}(900°C)}\right)^{\frac{1}{2}} * \left(\frac{M_{H_2O}}{M_{N_2}}\right)^{\frac{1}{4}}\right]^2 = 0.8124$$

$$\Phi_{H_2O,N_2} = \frac{1}{2\sqrt{2}} * \left(1 + \frac{M_{H_2O}}{M_{N_2}}\right)^{-\frac{1}{2}} * \left[1 + \left(\frac{\mu_{H_2O}(900°C)}{\mu_{N_2}(900°C)}\right)^{\frac{1}{2}} * \left(\frac{M_{N_2}}{M_{H_2O}}\right)^{\frac{1}{4}}\right]^2 = 1.206$$

$$\mu_{g,900°C} = \frac{X_{N_2} * \mu_{N_2}(900°C)}{X_{H_2O} * \Phi_{N_2,H_2O} + X_{N_2} * \Phi_{H_2O,N_2}} + \frac{X_{H_2O} * \mu_{H_2O}(900°C)}{X_{H_2O} * \Phi_{N_2,H_2O} + X_{N_2} * \Phi_{H_2O,N_2}} = 44 * 10^{-6}$$

$\rho_{H_2O}(900°C) = 0.187164 \frac{kg}{m^3}$ $\rho_{N_2}(900°C) = 0.29087 \frac{kg}{m^3}$

$\dot{V}_{H_2O} = 400 \frac{mLn}{min}$ $\dot{V}_{N_2} = 500 \frac{mLn}{min}$

$$\rho_g = \frac{\frac{\rho_{H_2O}(900°C)}{\dot{V}_{H_2O}} + \frac{\rho_{N_2}(900°C)}{\dot{V}_{N_2}}}{\dot{V}_{N_2} + \dot{V}_{H_2O}} = 0.025 \frac{g}{cm^3}$$

$d_{sv} = 180 \mu m$ $\rho_P = 3.2 \frac{g}{cm^3}$ $g = 9.81 \frac{m}{s^2}$

$$Ar = \frac{\rho_G * d_{sv}^3 * (\rho_P - \rho_g) * g}{\mu_{g,900°C}^2} = 22.95$$

$$U_{mf} = \frac{\mu_{g,900°C}}{\rho_g * d_{sv}} * \left(\sqrt{33.7^2 + 0.0408 * Ar} - 33.7\right) = 0.016 \frac{m}{s}$$